

Engineering Seismology and Seismic Hazard – 2019

Lecture 17

Ground Motion Prediction Equations

Valerio Poggi

Seismological Research Center (CRS)

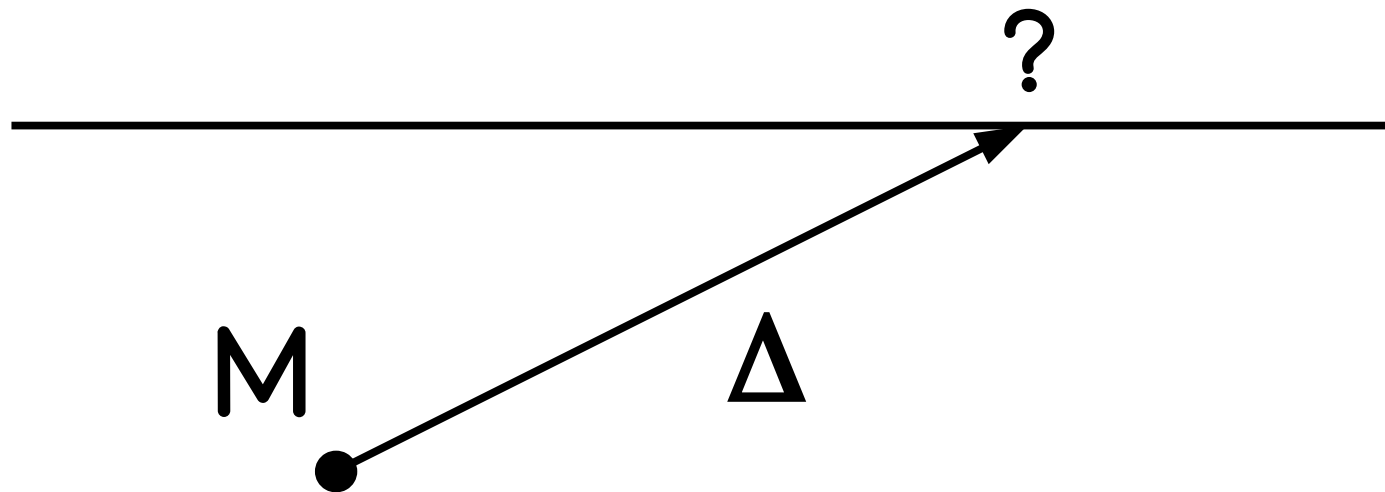
National Institute of Oceanography and Applied Geophysics (OGS)



Ground Motion Prediction

Ground Motion Prediction Equations (GMPEs) are the simplest **empirical** (and in few cases analytical) answer to the following question:

“If we know where a major earthquake is likely to occur, how large will the ground motion be at a particular site?”

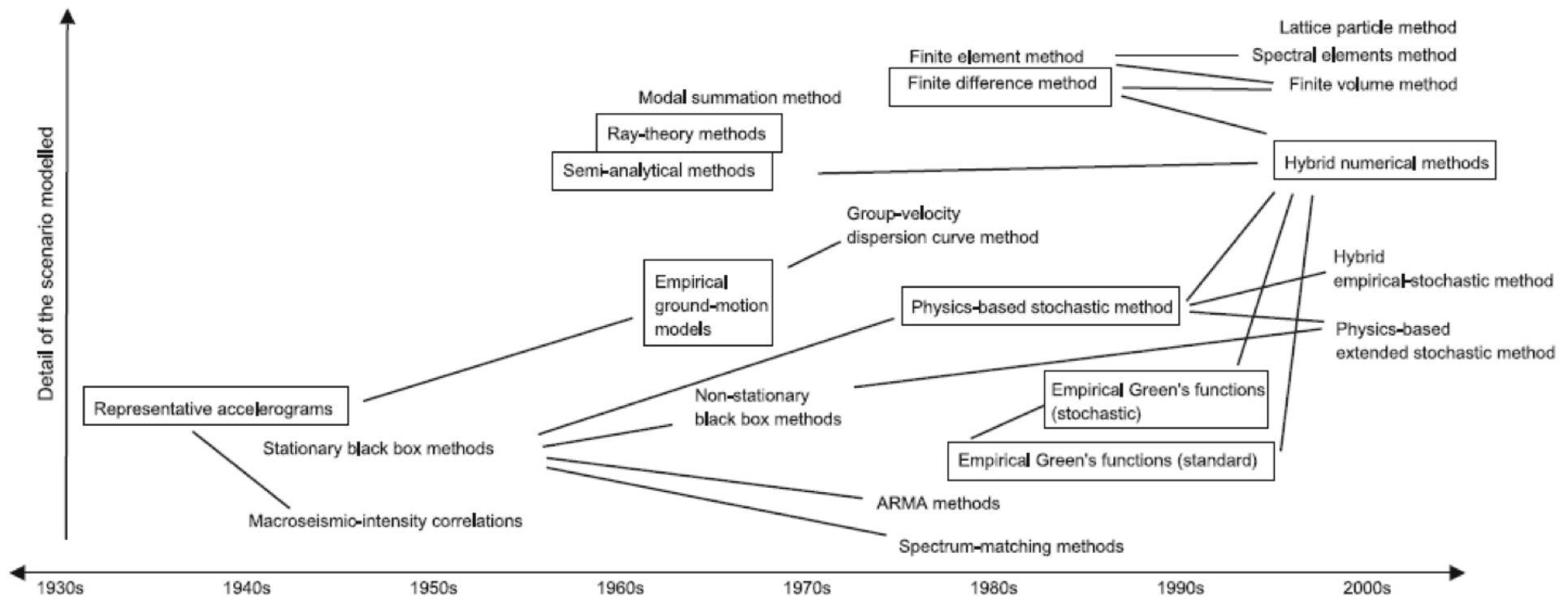


$$\log(Y) = f(M, \Delta, \dots) + E$$

History of Ground Motion Prediction

Empirical models still the basis of almost all PSHAs (except in stable low-seismicity regions)

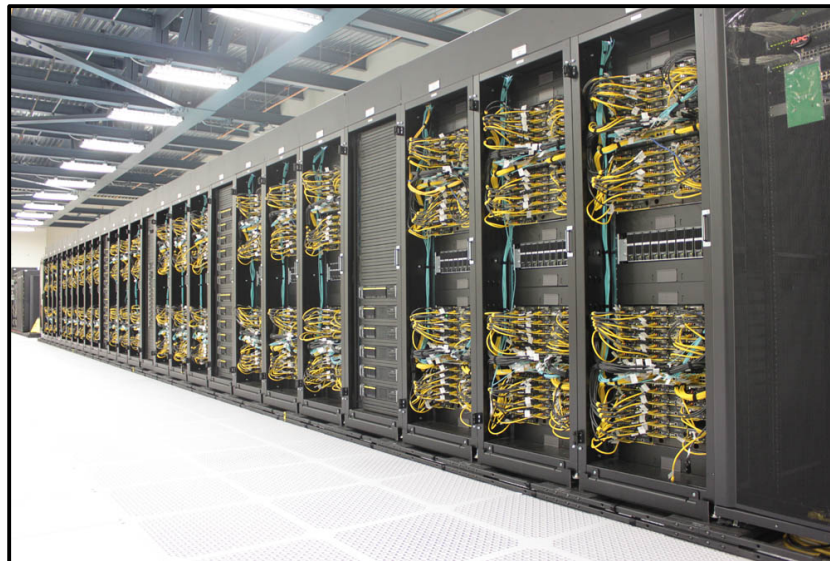
Boxes indicate those methods often used in research and/or practice



Prediction vs Simulation

Why an empirical prediction? Ground motion could also be estimated by numerical simulation. However...

1) Numerical simulation is computationally expensive and does not (directly) provide estimates of the uncertainty. It also requires many parameters of difficult calibration.

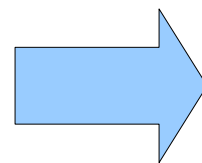
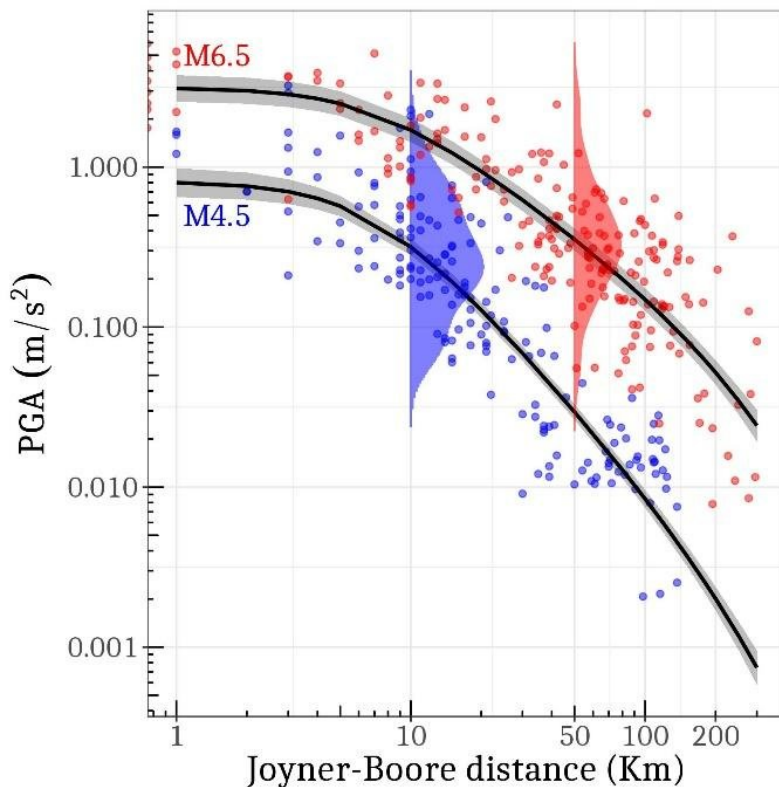


Nonetheless, simulated ground motion at the end still needs to be compared with actual data!

Prediction vs Simulation

2) Engineers need a fast, simple and cost effective approach to be used massively, as in Probabilistic Seismic Hazard Analysis.

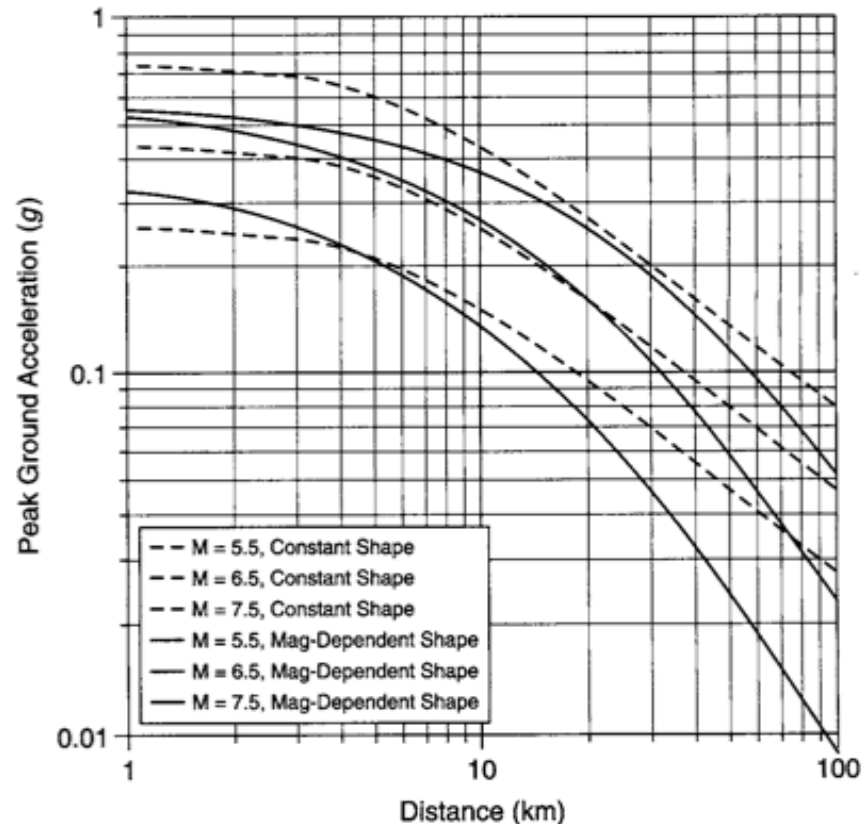
They also need a reliable assessment of the **prediction uncertainty**, which is often more important than accuracy of the mean estimate.



$$\log(Y) = f(M, \Delta, \dots) + E$$

Prediction Variables

- (1) Intensity or Magnitude (M_L , m_b , M_s , M_w)
- (2) Distance, using different metrics (R_{rup} , R_{jb} , R_{hypo} , R_{epi} ...)
- (3) Site term, generally by proxy (V_{s30} , f_0)
- (4) Faulting style and mechanism (strike-slip, normal, reverse)
- (5) Fault orientation and geometry
- (6) Focal depth
- (7) Others....



Ground Parameters

Predicted ground motion can be expressed in term of:

- PGA, PGV
- PSA, PSV
- Intensity
- Actual ground acceleration and velocity (rarely)
- Duration (as accessory parameter)

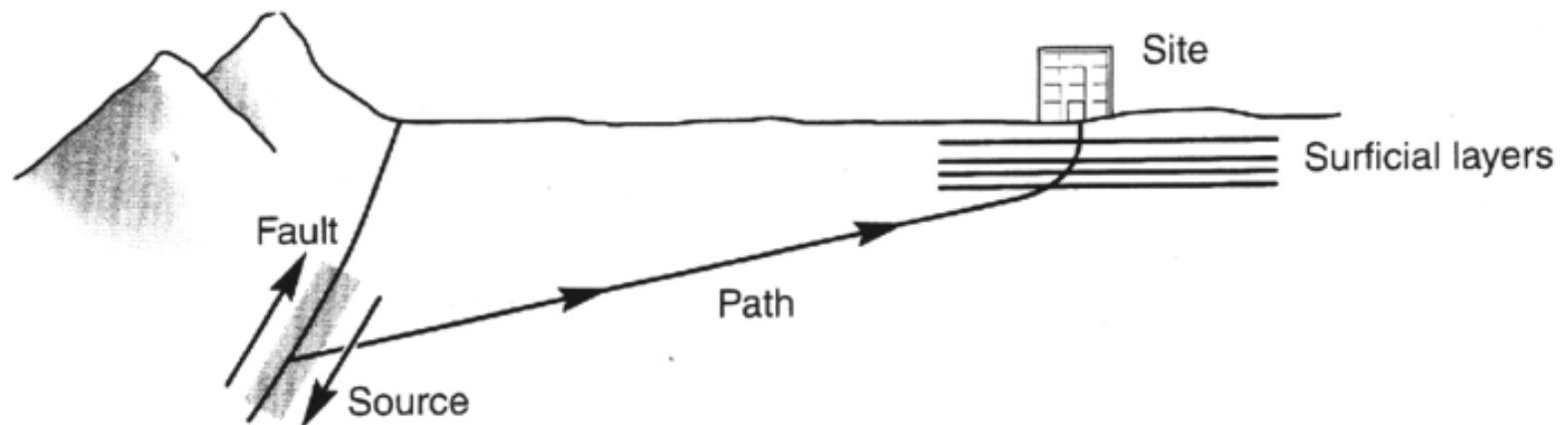
A combination of the horizontal components is usually considered, such as:

- Arithmetic mean
- Geometric mean
- Largest component
- Random

Source-Path-Site Components

Ground motion at any site can be seen as the combination of three contributions:

- Source characteristics (fault size, magnitude, seismic moment, etc)
- Wave propagation (geometrical and anelastic attenuation, scattering and dispersion),
- Site amplification due to both the site response and the other effects



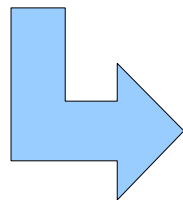
$$\text{GM Amplitude} = \text{Source term} * \text{Path term} * \text{Site term}$$

GMPE Functional Form

The functional form of empirical ground motion model is created following physical principles i.e. trying to reproduce the basic physics of the process.

Here is an “simple” example:

$$\log(Y) = c_0 + c_1 M + c_2 M^2 + c_3 \log(\sqrt{(R^2 + h^2)}) + \sigma$$



Different set of coefficients are defined for each ground motion measure type.

Table 2
Coefficients of Equation (1)

PSA at Frequency	c_0	c_1	c_2	c_3	σ -intra	σ -inter	σ -total
0.2	-4.374	1.134	0.0038	-1.426	0.26	0.17	0.31
0.33	-3.869	1.110	0.0039	-1.447	0.25	0.21	0.33
0.5	-4.503	1.532	-0.0430	-1.404	0.25	0.22	0.33
1	-2.009	1.890	-0.1248	-1.828	0.27	0.21	0.34
2	-4.128	1.792	-0.0791	-1.526	0.30	0.19	0.35
3.33	-2.076	1.889	-0.1257	-1.886	0.31	0.18	0.36
5	-3.918	2.112	-0.1266	-1.591	0.31	0.20	0.37
10	-2.839	1.905	-0.1134	-1.658	0.30	0.25	0.39
20	-2.337	1.902	-0.1252	-1.838	0.29	0.29	0.41
33	-2.313	1.840	-0.1119	-1.708	0.29	0.26	0.39
PGA	-2.427	1.877	-0.1214	-1.806	0.29	0.24	0.37
PGV	-4.198	1.818	-0.1009	-1.721	0.28	0.18	0.33

Equation (1) predicts 5% damped horizontal-component pseudospectral acceleration (PSA, in cm/s^2) for B/C site conditions, peak ground acceleration (PGA, in cm/s^2), and peak ground velocity (PGV, in cm/s). The standard deviation of residuals (σ -total) and its intraevent and interevent components are also given.

GMPE Functional Form

More recent GMPEs are far more complex and can have tens of coefficients!

$$\begin{aligned} \ln y_{ref} &= c_1 + \left\{ c_{1a} + \frac{c_{1c}}{\cosh[2 \max(M - 4.5, 0)]} \right\} F_{RV} + \left\{ c_{1b} + \frac{c_{1d}}{\cosh[2 \max(M - 4.5, 0)]} \right\} F_{NM} \\ &+ \left\{ c_7 + \frac{c_{7b}}{\cosh[2 \max(M - 4.5, 0)]} \right\} \Delta Z_{TOR} + \left\{ c_{11} + \frac{c_{11b}}{\cosh[2 \max(M - 4.5, 0)]} \right\} (\cos \delta)^2 \\ &+ c_2(M - 6) + \frac{c_2 - c_3}{c_n} \ln \left[1 + e^{c_n(c_M - M)} \right] + c_4 \ln \{ r_{rup} + c_5 \cosh[c_6 \max(M - c_{HM}, 0)] \} \\ &+ (c_{4a} - c_4) \ln \sqrt{r_{rup}^2 + c_{RB}^2} + \left\{ c_{71} + \frac{c_{72}}{\cosh[\max(M - c_{73}, 0)]} \right\} r_{rup} \\ &+ c_8 \max \left[1 - \frac{\max(r_{rup} - 40, 0)}{30}, 0 \right] \min \left[\frac{\max(M - 5.5, 0)}{0.8}, 1 \right] e^{-c_{8a}(M - c_{8b})^2} \Delta DPP \\ &+ c_9 F_{HW} \cos \delta \left[c_{9a} + (1 - c_{9a}) \tanh \left(\frac{R_x}{c_{9b}} \right) \right] \left[1 - \frac{\sqrt{r_{3b}^2 + Z_{TOR}^2}}{r_{rup} + 1} \right] \\ \ln y &= \ln y_{ref} + \phi_1 \min \left[\ln \left(\frac{V_{s,30}}{1130} \right), 0 \right] \\ &\phi_2 \left\{ e^{\phi_3[\min(V_{s,30}, 1130) - 360]} - e^{\phi_3(1130 - 360)} \right\} \ln \left(\frac{y_{ref} + \phi_4}{\phi_4} \right) \\ &\phi_5 \left(1 - e^{-\Delta Z_{TOR} / \phi_6} \right) \\ \Delta Z_{TOR} &= Z_{TOR} - E[Z_{TOR}] \\ E[Z_{TOR}] &= \max[2.704 - 1.226 \max(M - 5.849, 0), 0]^2 \text{ for reverse} \\ E[Z_{TOR}] &= \max[2.673 - 1.136 \max(M - 4.970, 0), 0]^2 \text{ For strike-slip/normal} \end{aligned}$$

Chiou and Youngs 2014

Abrahamson and Silva 2009

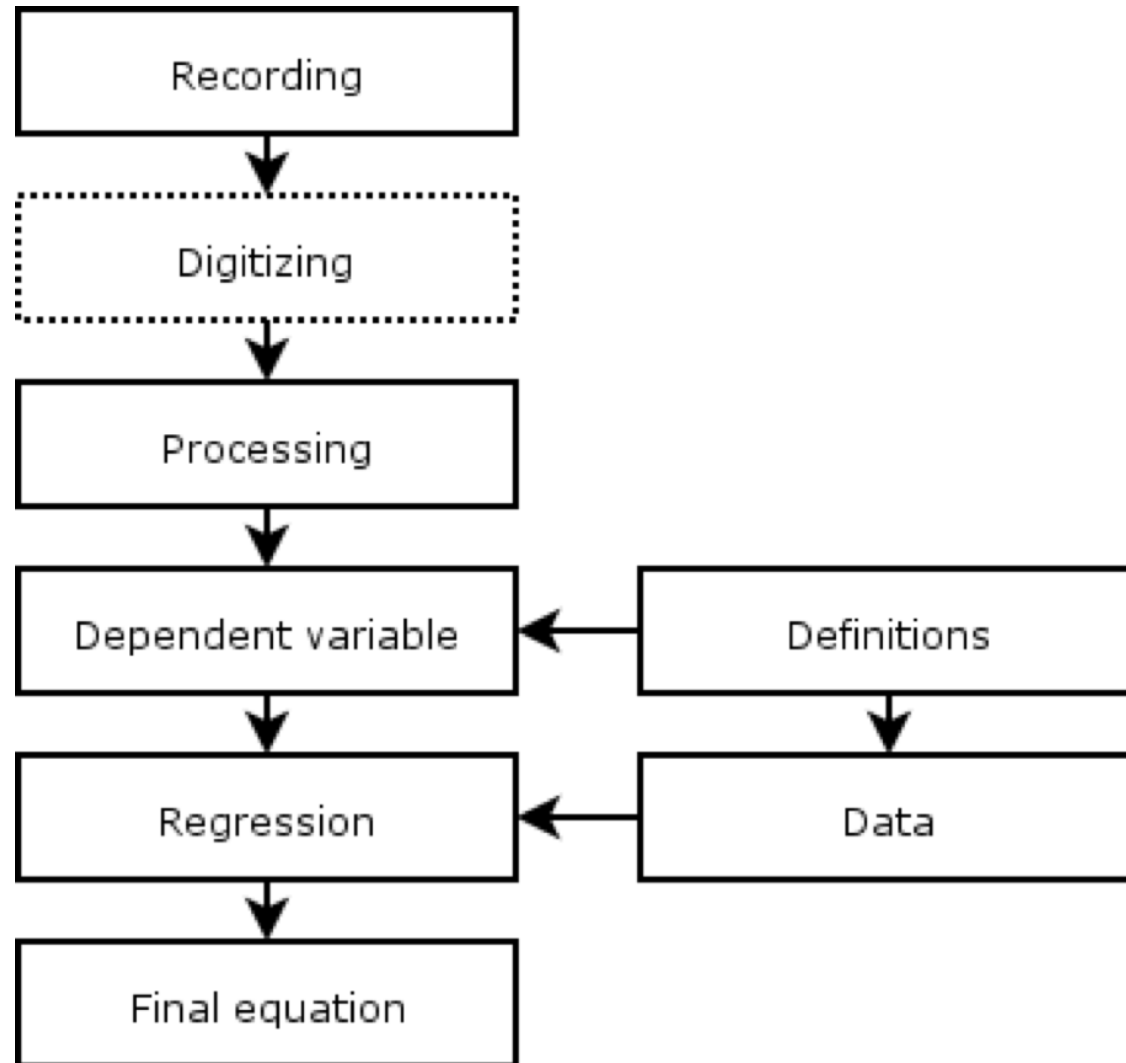
$$\begin{aligned} \ln Sa(g) &= f_1(M, R_{rup}) + a_{12}F_{RV} + a_{13}F_{NM} + a_{15}F_{AS} + f_5(\widehat{PGA}_{1100}, V_{S30}) \\ &+ F_{HW}f_4(R_{jb}, R_{rup}, R_x, W, \delta, Z_{TOR}, M) + f_6(Z_{TOR}) + f_8(R_{rup}, M) \\ &+ f_{10}(Z_{1.0}, V_{S30}) \\ f_1(M, R_{rup}) &= \begin{cases} a_1 + a_4(M - c_1) + a_8(8.5 - M)^2 + [a_2 + a_3(M - c_1)] \ln(R) & \text{for } M \leq c_1 \\ a_1 + a_5(M - c_1) + a_8(8.5 - M)^2 + [a_2 + a_3(M - c_1)] \ln(R) & \text{for } M > c_1 \end{cases} \\ R &= \sqrt{R_{rup}^2 + c_4^2} \\ f_5(\widehat{PGA}_{1100}, V_{S30}) &= \begin{cases} a_{10} \ln \left(\frac{V_{S30}}{V_{LIN}} \right) - b \ln(\widehat{PGA}_{1100} + c) \\ + b \ln \left(\widehat{PGA}_{1100} + c \left(\frac{V_{S30}}{V_{LIN}} \right)^n \right) & \text{for } V_{S30} < V_{LIN} \\ (a_{10} + bn) \ln \left(\frac{V_{S30}}{V_{LIN}} \right) & \text{for } V_{S30} \geq V_{LIN} \end{cases} \\ \text{where } V_{S30}^* &= \begin{cases} V_{S30} & \text{for } V_{S30} < V_1 \\ V_1 & \text{for } V_{S30} \geq V_1 \end{cases} \\ \text{and } V_1 &= \begin{cases} 1500 & \text{for } T \leq 0.50 \text{ s} \\ \exp[8.0 - 0.795 \ln(T/0.21)] & \text{for } 0.50 < T \leq 1 \text{ s} \\ \exp[6.76 - 0.297 \ln(T)] & \text{for } 1 < T < 2 \text{ s} \\ 700 & \text{for } T \geq 2 \text{ s} \end{cases} \\ f_4(R_{jb}, R_{rup}, \delta, Z_{TOR}, M, W) &= a_{14}T_1(R_{jb})T_2(R_x, W, \delta)T_3(R_x, Z_{TOR})T_4(M)T_5(\delta) \\ \text{where } T_1(R_{jb}) &= \begin{cases} 1 - \frac{R_{jb}}{30} & \text{for } R_{jb} < 30 \text{ km} \\ 0 & \text{for } R_{jb} \geq 30 \text{ km} \end{cases} \\ T_2(R_x, W, \delta) &= \begin{cases} 0.5 + \frac{R_x}{2W \cos(\delta)} & \text{for } R_x \leq W \cos(\delta) \\ 1 & \text{for } R_x > W \cos(\delta) \text{ or } \delta = 90^\circ \end{cases} \\ T_3(R_x, Z_{TOR}) &= \begin{cases} 1 & \text{for } R_x \geq Z_{TOR} \\ \frac{R_x}{Z_{TOR}} & \text{for } R_x < Z_{TOR} \end{cases} \\ T_4(M) &= \begin{cases} 0 & \text{for } M \leq 6 \\ M - 6 & \text{for } 6 < M < 7 \\ 1 & \text{for } M \geq 7 \end{cases} \\ T_5(\delta) &= \begin{cases} 1 - \frac{\delta - 30}{60} & \text{for } \delta \geq 30 \\ 1 & \text{for } \delta < 30 \end{cases} \\ f_6(Z_{TOR}) &= \begin{cases} \frac{a_{16}Z_{TOR}}{10} & \text{for } Z_{TOR} < 10 \text{ km} \\ a_{16} & \text{for } Z_{TOR} \geq 10 \text{ km} \end{cases} \\ f_8(R_{rup}, M) &= \begin{cases} 0 & \text{for } R_{rup} < 100 \text{ km} \\ a_{18}(R_{rup} - 100)T_6(M) & \text{for } R_{rup} \geq 100 \text{ km} \end{cases} \\ \text{where } T_6(M) &= \begin{cases} 1 & \text{for } M < 5.5 \\ 0.5(6.5 - M) + 0.5 & \text{for } 5.5 \leq M \leq 6.5 \\ 0.5 & \text{for } M > 6.5 \end{cases} \\ f_{10}(Z_{1.0}, V_{S30}) &= a_{21} \ln \left(\frac{Z_{1.0} + c_2}{Z_{1.0}(V_{S30}) + c_2} \right) + \begin{cases} a_{22} \ln \left(\frac{Z_{1.0}}{200} \right) & \text{for } Z_{1.0} \geq 200 \\ 0 & \text{for } Z_{1.0} < 200 \end{cases} \\ \text{where } \ln[Z_{1.0}(V_{S30})] &= \begin{cases} 6.745 & \text{for } V_{S30} < 180 \text{ m/s} \\ 6.745 - 1.35 \ln \left(\frac{V_{S30}}{180} \right) & \text{for } 180 \leq V_{S30} \leq 500 \text{ m/s} \\ 5.394 - 4.48 \ln \left(\frac{V_{S30}}{500} \right) & \text{for } V_{S30} > 500 \text{ m/s} \end{cases} \\ a_{21} &= \begin{cases} 0 & \text{for } V_{S30} \geq 1000 \\ -\frac{(a_{10} + bn) \ln \left(\frac{V_{S30}}{\min(V_1, 1000)} \right)}{\ln \left(\frac{Z_{1.0} + c_2}{Z_{1.0} + c_2} \right)} & \text{for } (a_{10} + bn) \ln \left(\frac{V_{S30}}{\min(V_1, 1000)} \right) + e_2 \ln \left(\frac{Z_{1.0} + c_2}{Z_{1.0} + c_2} \right) < 0 \\ e_2 & \text{otherwise} \end{cases} \\ e_2 &= \begin{cases} 0 & \text{for } T < 0.35 \text{ s or } V_{S30} > 1000 \\ -0.25 \ln \left(\frac{V_{S30}}{1000} \right) \ln \left(\frac{T}{0.35} \right) & \text{for } 0.35 \leq T \leq 2 \text{ s} \\ -0.25 \ln \left(\frac{V_{S30}}{1000} \right) \ln \left(\frac{2}{0.35} \right) & \text{for } T > 2 \text{ s} \end{cases} \\ a_{22} &= \begin{cases} 0 & \text{for } T < 2 \text{ s} \\ 0.0625(T - 2) & \text{for } T \geq 2 \text{ s} \end{cases} \end{aligned}$$

Implementation Workflow

Classical procedure used to derive a GMPE (from Douglas, 2003):

- Earthquakes are recorded using strong-motion instruments to get a set of records for analysis.
- If the earthquakes were recorded on analogue accelerographs, which use paper or film, then the accelerograms are digitized to get the data into a form usable for numerical analysis.
- The digitized strong-motion records are processed to remove short- and long-period noise, which is introduced in the recording and digitization stages. This processing usually consists of fitting a zero baseline to the record and then applying a bandpass filter.
- A dependent variable is selected and calculated from the strong-motion records. This dependent variable, such as peak ground acceleration or spectral acceleration, should be useful for seismic design and analysis.
- Independent variables, such as magnitude and source-to-site distance, that characterise the strong-motion records in the data set are then collected for all the time-histories used.
- Regression analysis is performed to derive equations to estimate the dependent variable (a strong-motion parameter) given the independent variables. At the same time, the standard deviation of the equations are calculated.
- The derived equations are used in seismic hazard analysis, either deterministic or probabilistic, to give estimates of the strong ground motion that could be expected at a site during a future earthquake.

Implementation Workflow



Strong Motion Databases

ITACA is the Italian on-line Strong Motion Archive.

It contains more than 2000 three component waveforms (corrected and uncorrected) generated by more than 1000 earthquakes.

<http://itaca.mi.ingv.it/ItacaNet/>

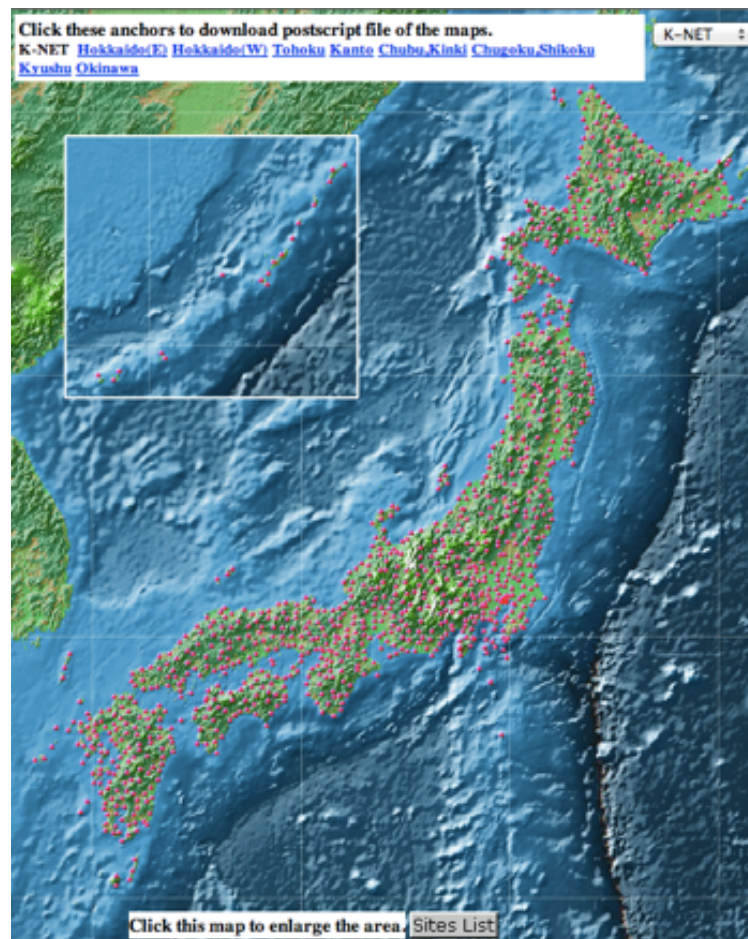


The screenshot shows the ITACA web interface. On the left is a navigation menu with options like Home, Info, Events, and Stations. The main area is titled 'Cerca eventi' (Search events) and contains search filters for 'Ricerca rapida', 'Parametri geofisici', and 'Parametri geografici'. Below the filters is a search form with fields for 'ID ITACA', 'Nome evento', 'Data', and 'Numero di registrazioni'. A 'Cerca' button is visible. To the right is a map showing 'Eventi sulla mappa: 1882' with red circles indicating event locations. Below the map is a table of selected events.

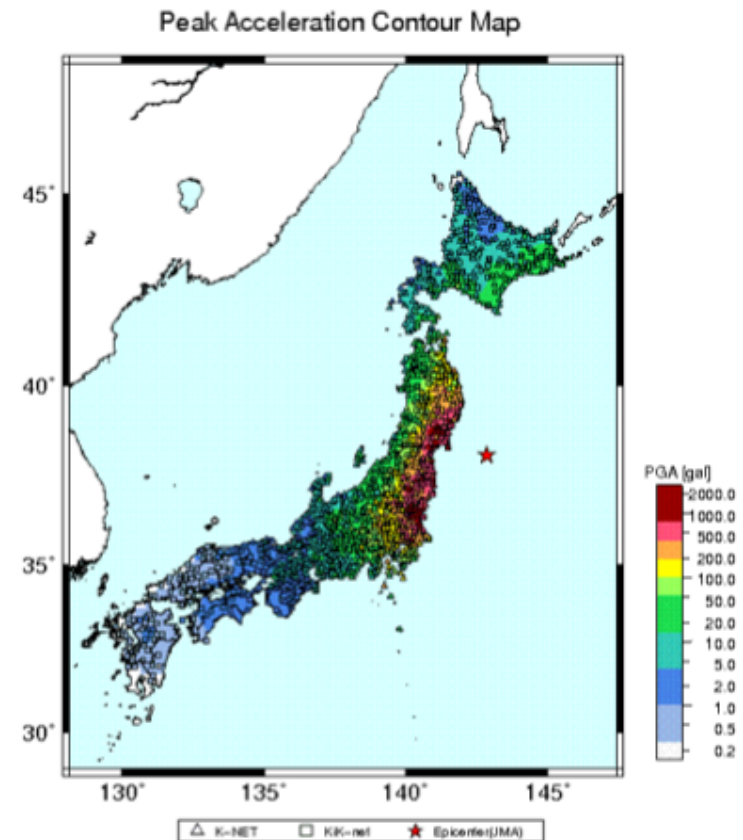
ID ITACA	Data	Nome evento	Nazione	Regione	Comune	Latitudine	Longitudine	Profondità [km]	ML	MW	Tipologia di faglia	Registrazioni
EMSC-20181226_0000014	2018-12-26 02:19:17	SICILY_ITALY	Italia	Sicilia	Viagrande	37.64400	15.11600		4.8	4.9	Trascorrente	46
EMSC-20181224_0000148	2018-12-24 19:26:18	SICILY_ITALY	Italia	Sicilia	Ragana	37.68800	14.96500	2.1	4			9
EMSC-20181224_0000128	2018-12-24 16:50:12	SICILY_ITALY	Italia	Sea or international waters		37.71600	15.03900	2.2	4.3			9
EMSC-20181224_0000075	2018-12-24 12:08:55	SICILY_ITALY	Italia	Sicilia	Zafferana Etnea	37.71800	15.03700	2.1	4			10
EMSC-20181130_0000088	2018-11-30 06:30:29	ADRIATIC_SEA		Sea or international waters		42.46000	16.27000	10	4.2			25
EMSC-20181126_0000065	2018-11-26 14:17:37	MONTENEGRO	Montenegro	Herceg Novi Municipality		42.54000	18.56000	10	4.2			1
EMSC-20181118_0000061	2018-11-18 12:48:43	NORTHERN_ITALY	Italia	Sea or international waters		44.05130	12.48580	36.8	4.2	4	Inverso/Sovrascorrimento	143
EMSC-20181006_0000002	2018-10-06 00:34:19	SICILY_ITALY	Italia	Sicilia		37.60880	14.93950	4.5	4.7	4.6	Trascorrente	65
EMSC-20180928_0000014	2018-09-28 05:24:30	SICILY_ITALY	Italia	Sea or international waters		38.38000	15.73000	11	4.2			51
EMSC-20180915_0000014	2018-09-15 03:09:13	CROATIA	Croazia	Sibensko-kninska županija		43.79000	15.78000	2	4.2			1

Strong Motion Databases

Kyoshin Net (**K-NET**) is the Japanese strong motion network
Probably the densest national strong-motion network in the
world, with more than 1000 stations.



<http://www.k-net.bosai.go.jp>

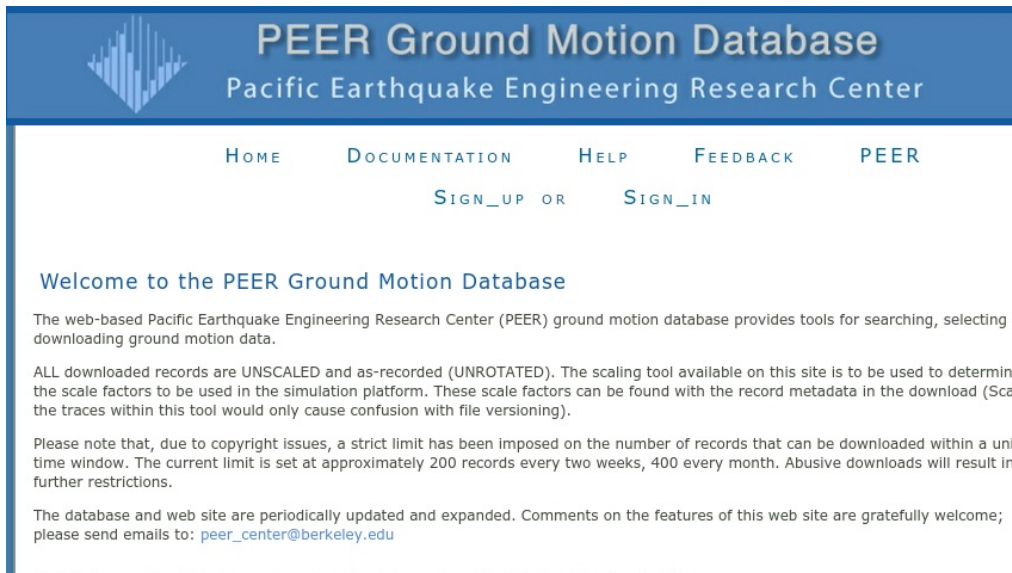


2011/03/11-14:46 38.103N 142.860E 24km M9.0

Strong Motion Databases

The Pacific Earthquake Engineering Research Center (**PEER**) provides a global database of homogeneously processed strong motion recordings for Shallow Crustal Earthquakes in Active Tectonic Regimes.

<http://peer.berkeley.edu>



PEER Ground Motion Database
Pacific Earthquake Engineering Research Center

HOME DOCUMENTATION HELP FEEDBACK PEER

SIGN_UP OR SIGN_IN

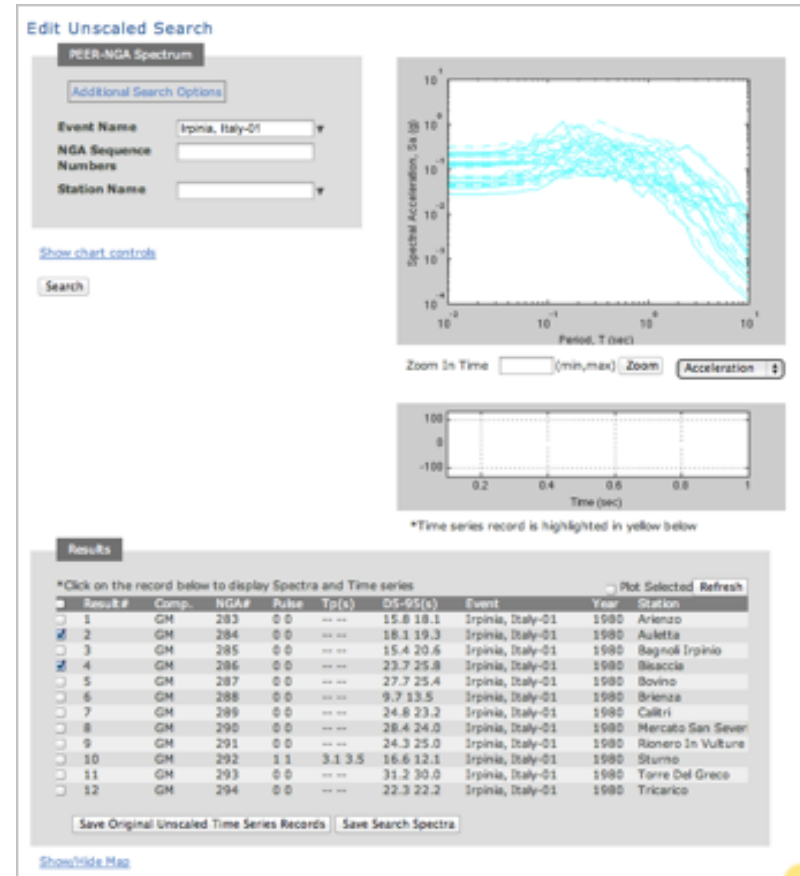
Welcome to the PEER Ground Motion Database

The web-based Pacific Earthquake Engineering Research Center (PEER) ground motion database provides tools for searching, selecting and downloading ground motion data.

ALL downloaded records are UNSCALED and as-recorded (UNROTATED). The scaling tool available on this site is to be used to determine the scale factors to be used in the simulation platform. These scale factors can be found with the record metadata in the download (Scaling the traces within this tool would only cause confusion with file versioning).

Please note that, due to copyright issues, a strict limit has been imposed on the number of records that can be downloaded within a unique time window. The current limit is set at approximately 200 records every two weeks, 400 every month. Abusive downloads will result in further restrictions.

The database and web site are periodically updated and expanded. Comments on the features of this web site are gratefully welcome; please send emails to: peer_center@berkeley.edu



Edit Unscaled Search

PEER-NGA Spectrum

Additional Search Options

Event Name: Irpinia, Italy-01
NGA Sequence Numbers:
Station Name:
[Show chart controls](#)

Results

*Click on the record below to display Spectra and Time series

Result#	Comp.	NGA#	Pulse	Tp(s)	DS-95(s)	Event	Year	Station
1	GM	283	0 0	---	15.8 18.1	Irpinia, Italy-01	1980	Arienzo
2	GM	284	0 0	---	18.1 19.3	Irpinia, Italy-01	1980	Auletta
3	GM	285	0 0	---	15.4 20.6	Irpinia, Italy-01	1980	Bagnoli Irpinio
4	GM	286	0 0	---	23.7 25.8	Irpinia, Italy-01	1980	Biaccio
5	GM	287	0 0	---	27.7 25.4	Irpinia, Italy-01	1980	Bovino
6	GM	288	0 0	---	9.7 13.5	Irpinia, Italy-01	1980	Brienza
7	GM	289	0 0	---	24.8 23.2	Irpinia, Italy-01	1980	Caltri
8	GM	290	0 0	---	28.4 24.0	Irpinia, Italy-01	1980	Mercato San Severo
9	GM	291	0 0	---	24.3 25.0	Irpinia, Italy-01	1980	Rosero In Valture
10	GM	292	1 1	3.1 3.5	16.6 12.1	Irpinia, Italy-01	1980	Storno
11	GM	293	0 0	---	31.2 30.0	Irpinia, Italy-01	1980	Torre Del Greco
12	GM	294	0 0	---	22.3 22.2	Irpinia, Italy-01	1980	Tricarico

[Show/Hide Map](#)

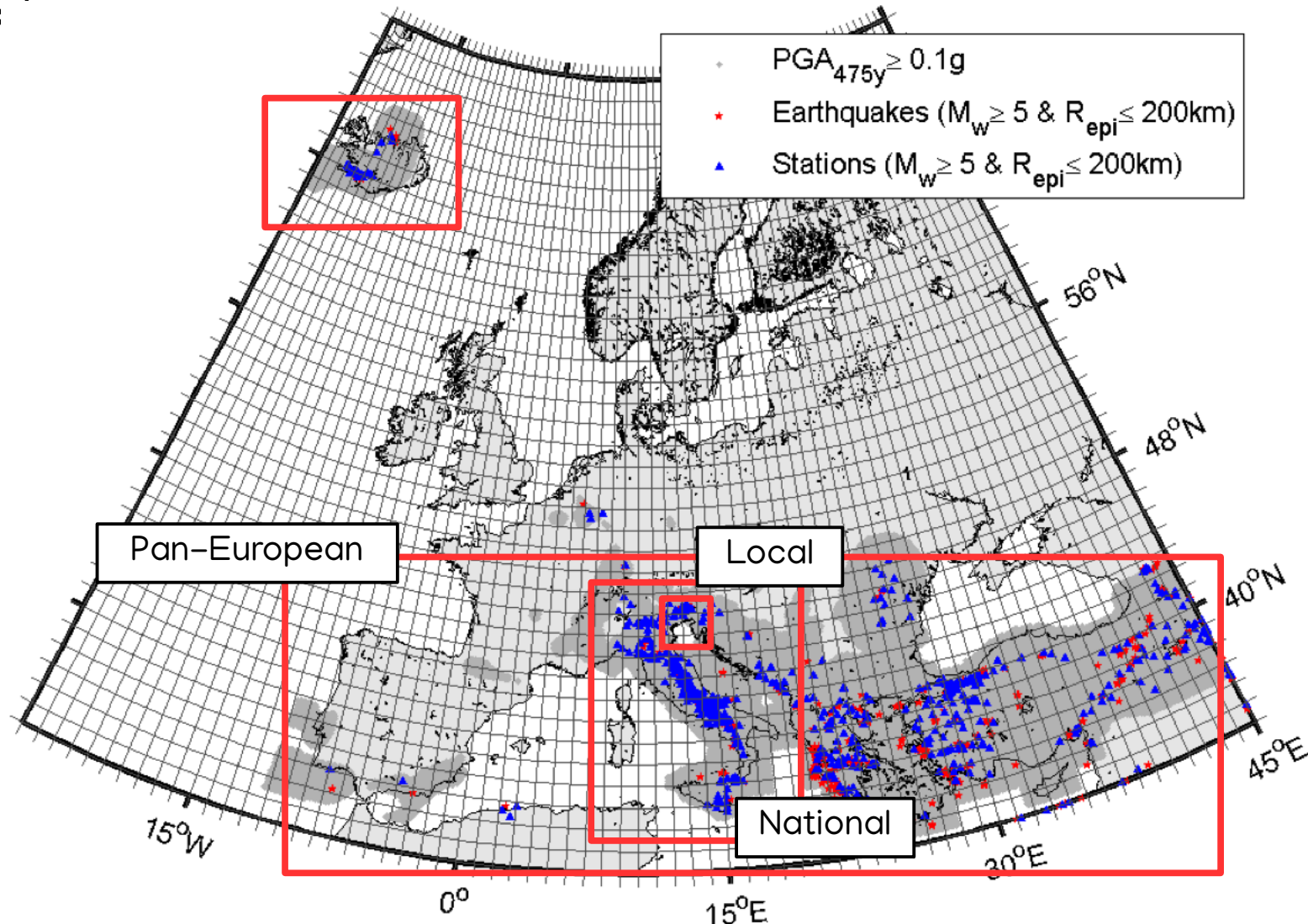
Figure 1: Spectral Acceleration vs. Period T (sec)
A log-log plot showing Spectral Acceleration (g) on the y-axis (ranging from 10⁻⁴ to 10¹) versus Period T (sec) on the x-axis (ranging from 10⁻² to 10¹). Multiple cyan lines represent different records, showing a peak in acceleration between 0.1 and 1.0 seconds.

Figure 2: Time series record
A plot showing Acceleration (g) on the y-axis (ranging from -100 to 100) versus Time (sec) on the x-axis (ranging from 0 to 1). The plot shows a single time series record highlighted in yellow.

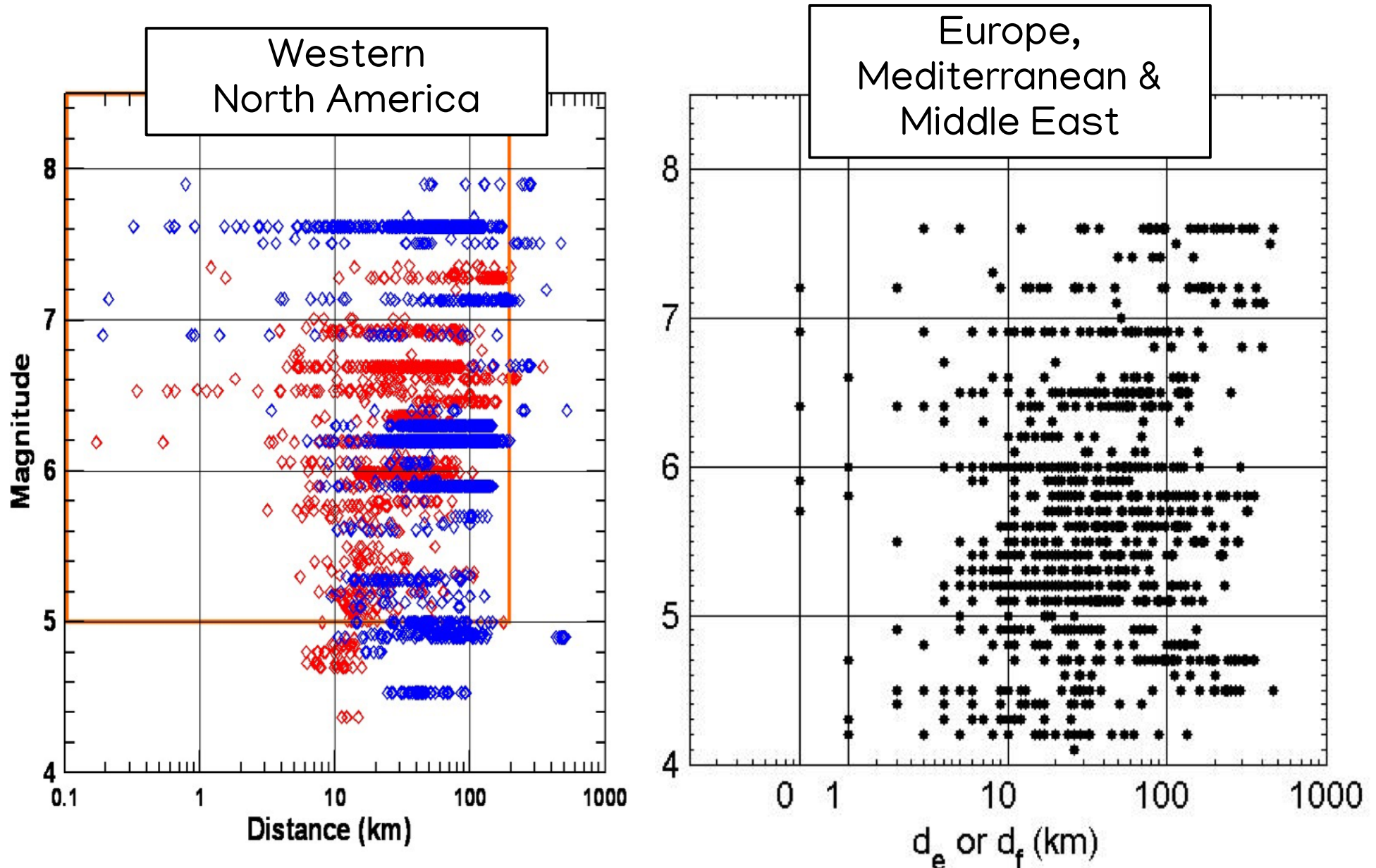
*Time series record is highlighted in yellow below

Available Data In Europe

Text



Regional M-D Distributions



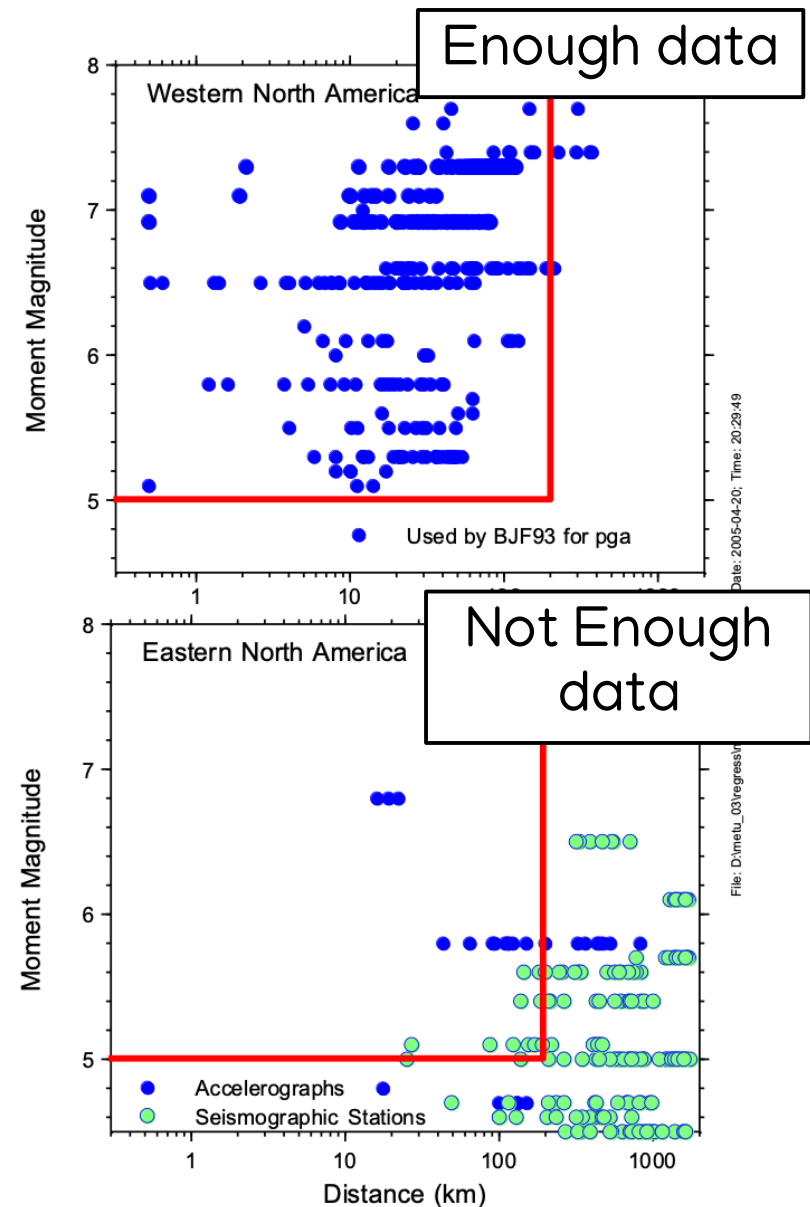
Empirical vs Simulation Data

1) When have data (rare for most of the world):

- Regression analysis of observed data

2) When adequate data are lacking:

- Regression analysis of simulated data (making use of motions from smaller events if available to constrain distance dependence of motions).
- Hybrid methods, capturing complex source effects from observed data and modifying for regional differences.



Data Regression

Two are the most common methodologies:

- Two step regression method (Joyner and Boore 1981; Joyner and Boore 1993, 1994) → **weighted least square**
- One-stage mixed-effects model regression algorithm (Abrahamson and Youngs, 1992) → **maximum likelihood**

Both these algorithms, in their current form, assume that the intraevent residuals are independent

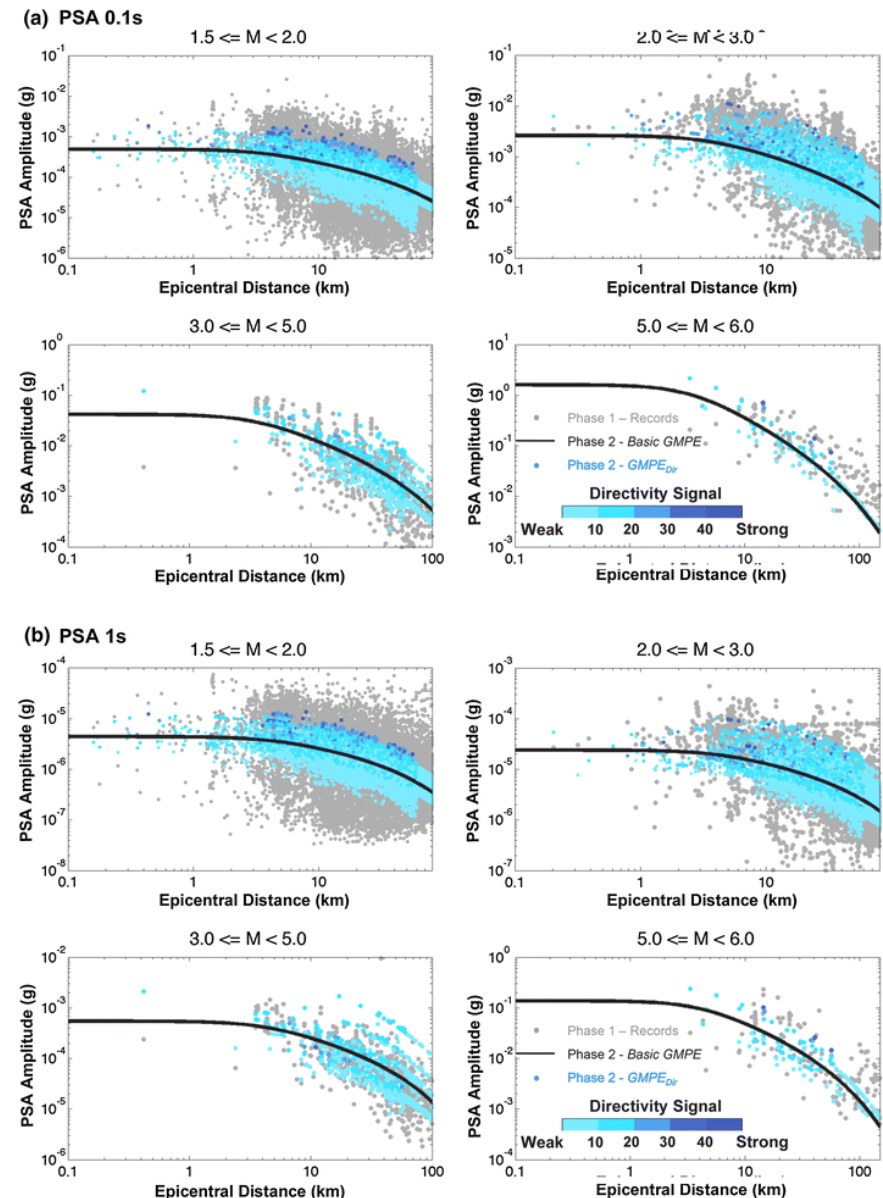
Simple regression techniques should generally be excluded unless they are capable to account for:

- The correlation between subsets of recordings (e.g. recordings for a single earthquake from many stations)
- The unbalancing in the dataset (e.g. each earthquake can have a different number of recordings available)

Data Regression

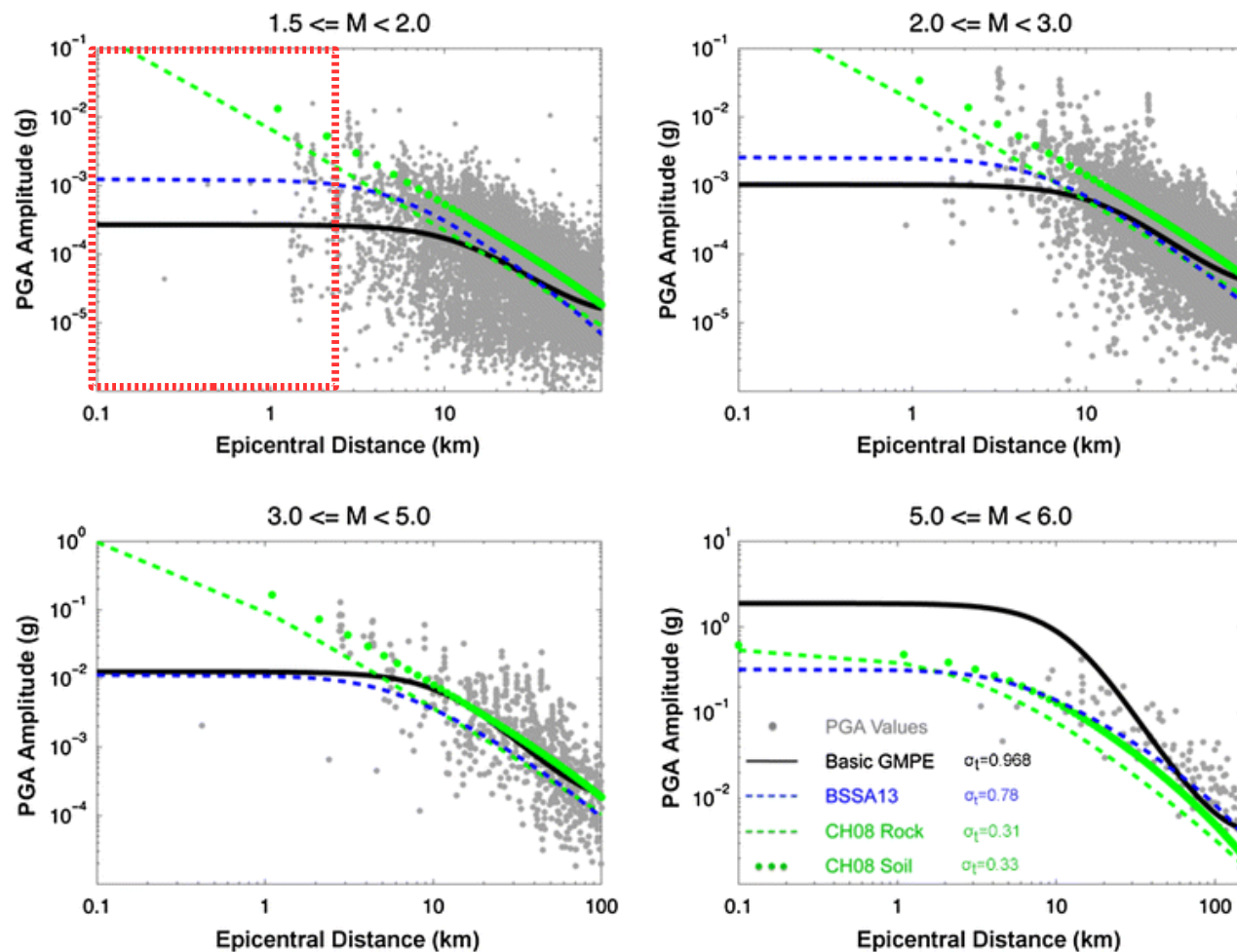
Remember that GMPE regression is a multidimensional fitting problem, depending on the number of predictor variables used.

Thus, it might be difficult to visualize!



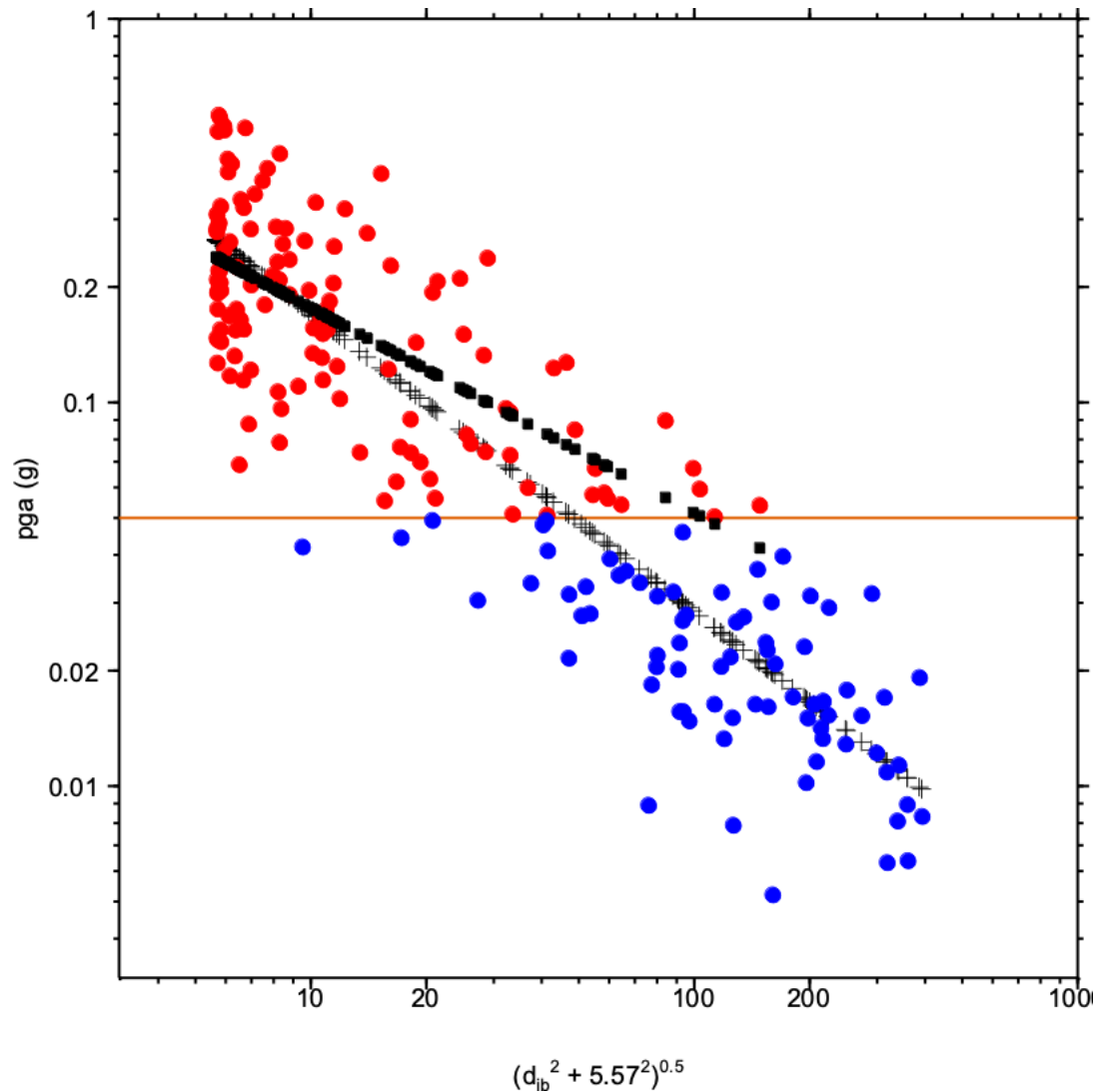
Errors: Lack of Data

Lack of data is particularly critical in the near-field. Extrapolation in this region can bring to significant errors in the prediction.



Errors: Effect of Triggering

Censoring of triggered data can lead to bias in coefficients



Recorded

Trigger Level of
Instrument
(e.g. 0.05g)

Not
Recorded

Effect of Magnitude

Source scaling theory predicts a general increase with magnitude for a fixed distance, with more sensitivity to magnitude for long periods and possible nonlinear dependence on magnitude.

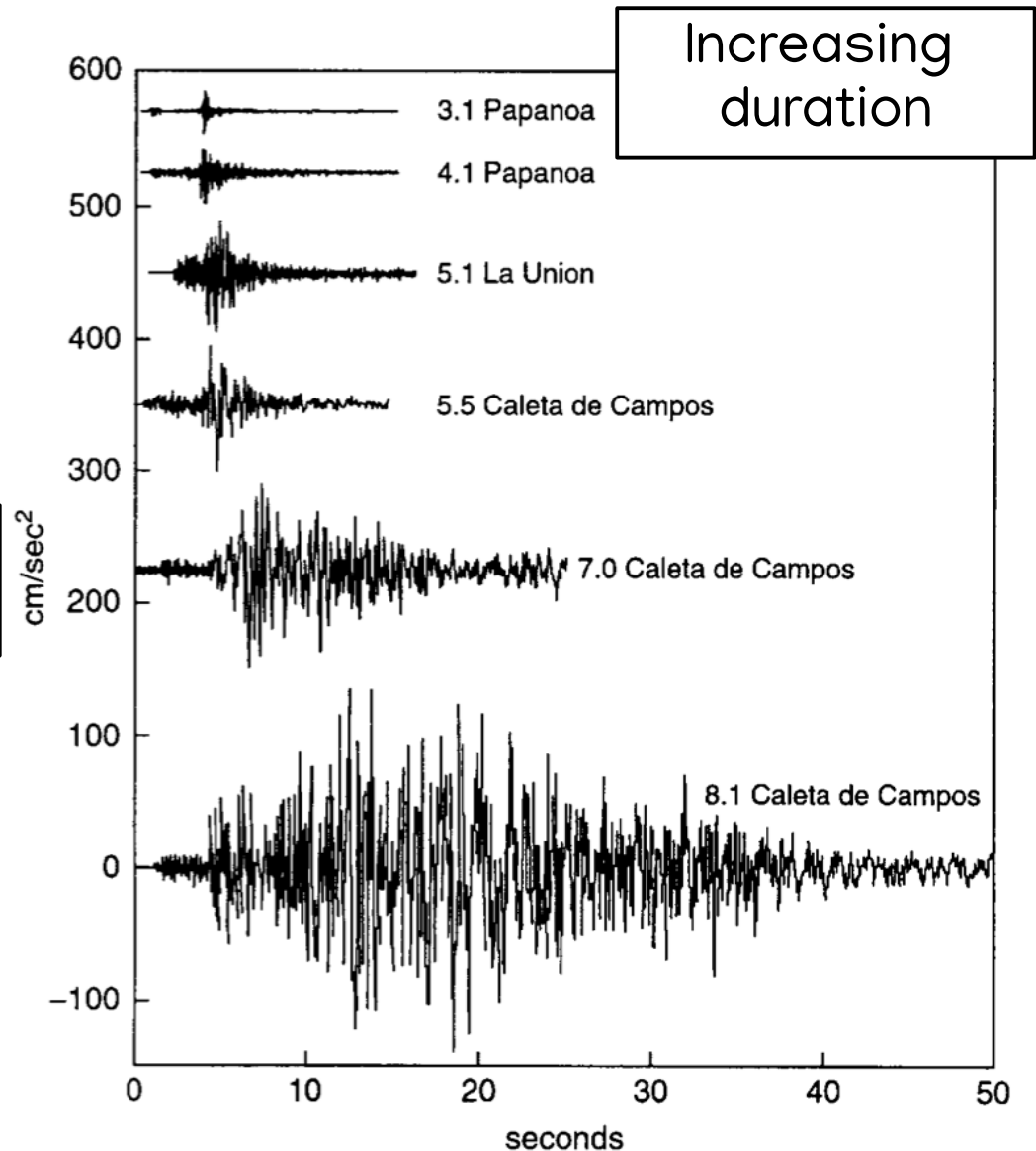
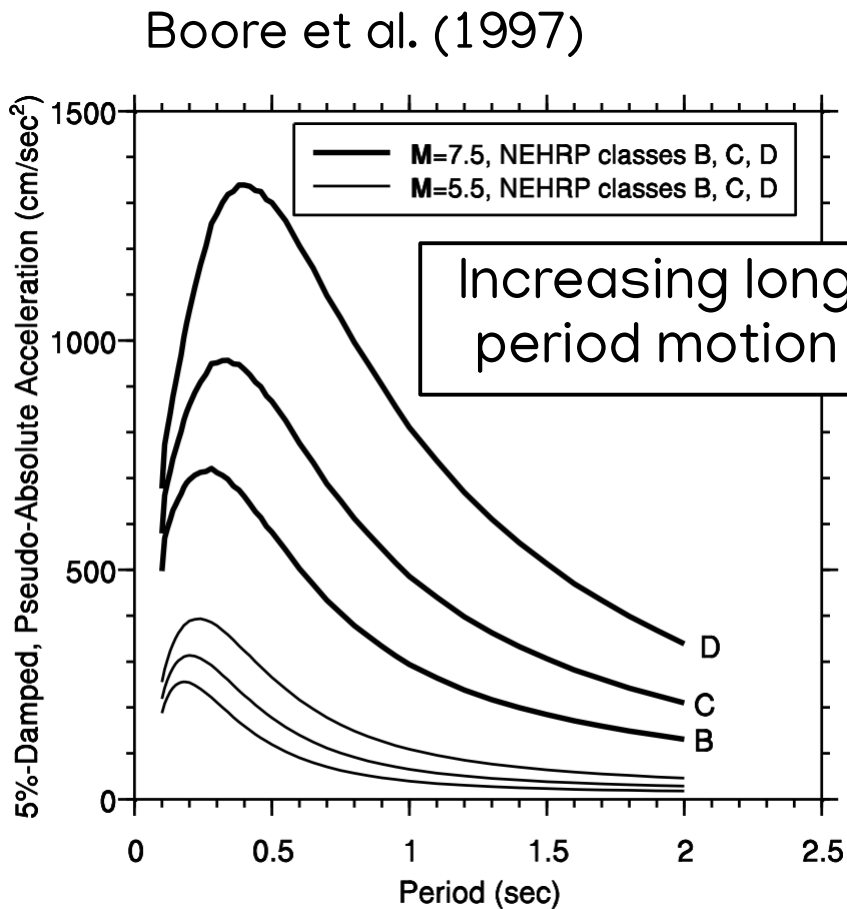
Of the different magnitude scales, the **Moment Magnitude** (M_w) is the most useful for prediction, because:

- Best single measure of overall size of an earthquake
- Base on non-saturated data
- Can be determined from ground deformation or seismic waves
- Can be estimated from paleoseismological studies
- Can be related to slip rates on faults

$$M_0 = \mu S A \quad \longrightarrow \quad M_w = \frac{2}{3} \log(M_0) - 10.7$$

Effect of Magnitude

Anderson & Quaes (1988)



Effect of Distance

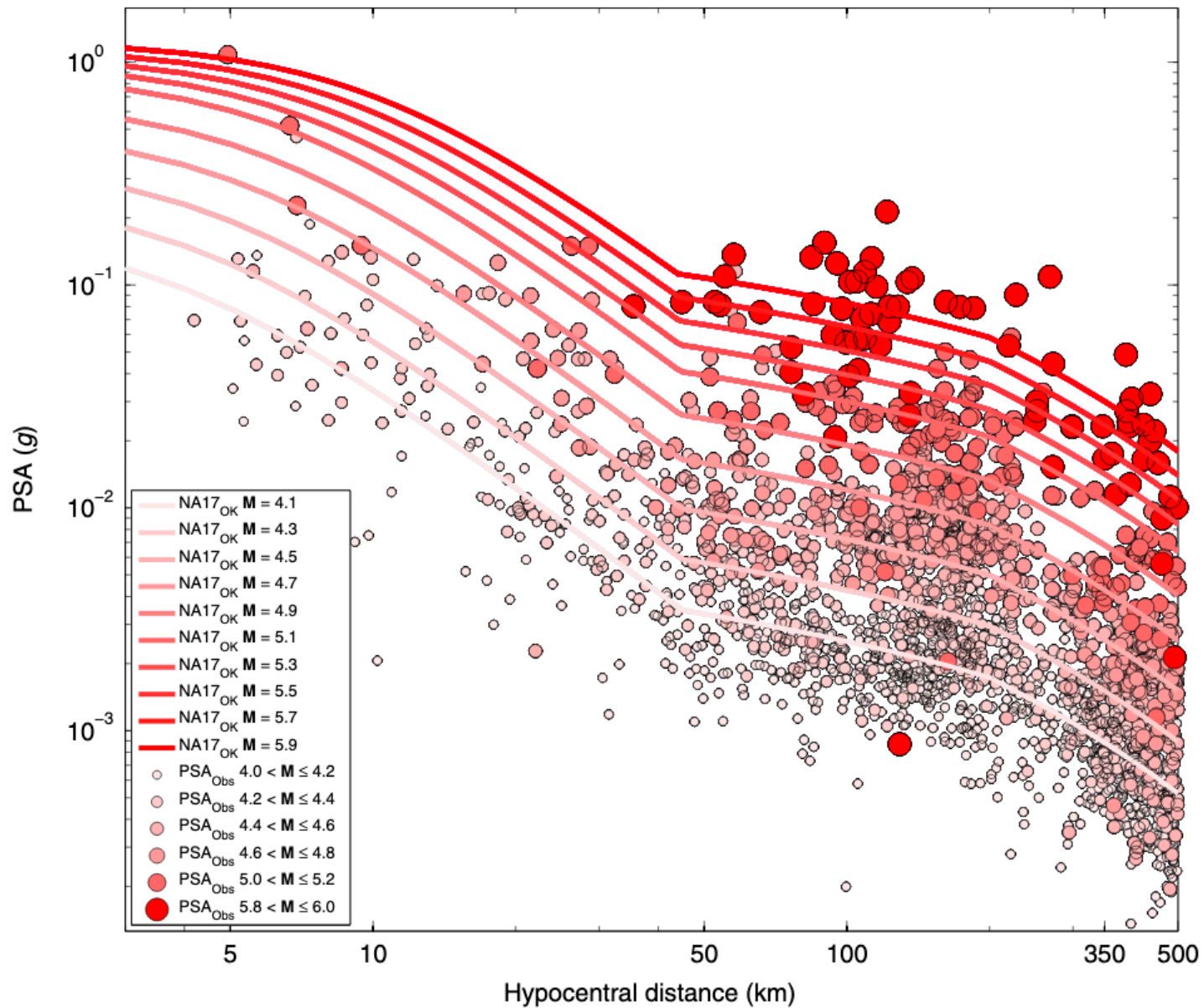
Generally, ground motion will decrease with distance (it will attenuate → that is why GMPE are also called attenuation functions) due to:

- Geometrical spreading ($1/r$ in uniform media)
- Intrinsic attenuation and scattering

Wave propagation in a heterogeneous earth predicts more complicated behavior e.g., increase at some distances due to critical angle reflections (“**Moho-bounce**”).

Equations assume average over various crustal structures.

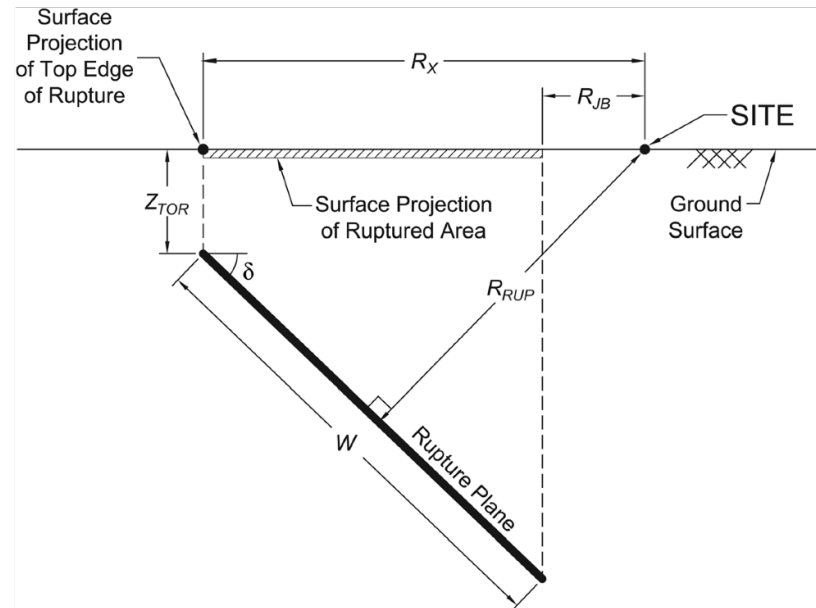
Effect of Distance



Distance Metrics

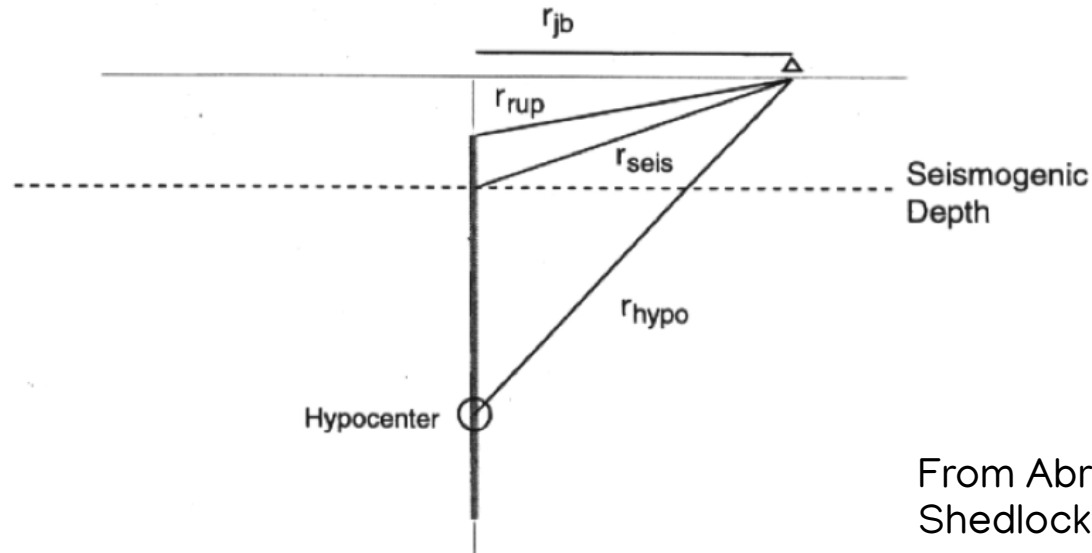
Many different measures of distance (**distance metrics**):

- R_{epi} → Epicentral distance
- R_{hypo} → Hypocentral (focal) distance
- R_{rup} → Rupture distance
- R_{jb} → Joyner–Boore distance, the distance to the vertical projection on the surface of the rupture
- R_{seis} → Seismogenic distance, the distance to the seismogenic part of the rupture



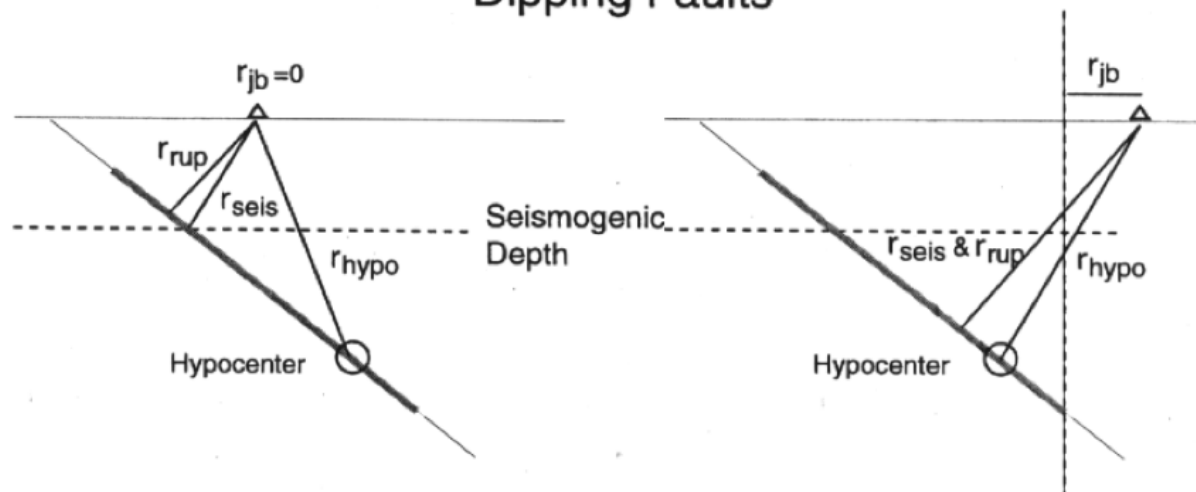
Distance Metric Examples

Vertical Faults



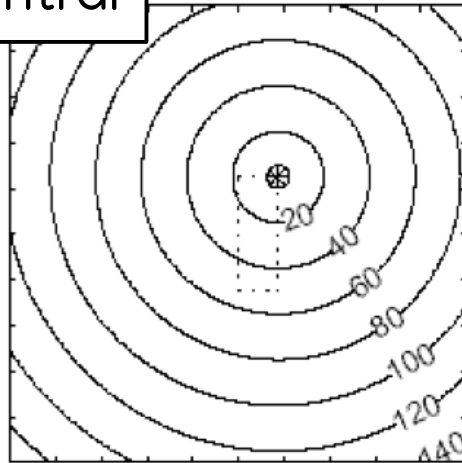
From Abrahamson and Shedlock, 1997

Dipping Faults

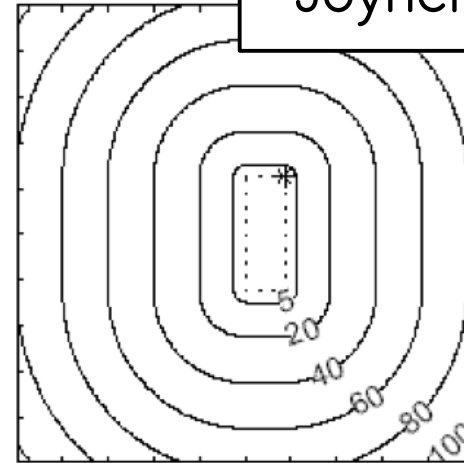


Spatial Pattern

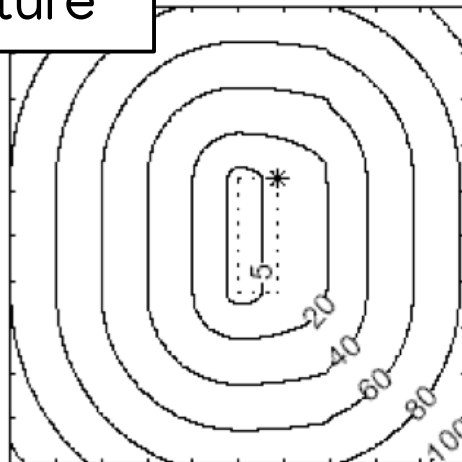
Epicentral



Joyner-Boore



Rupture

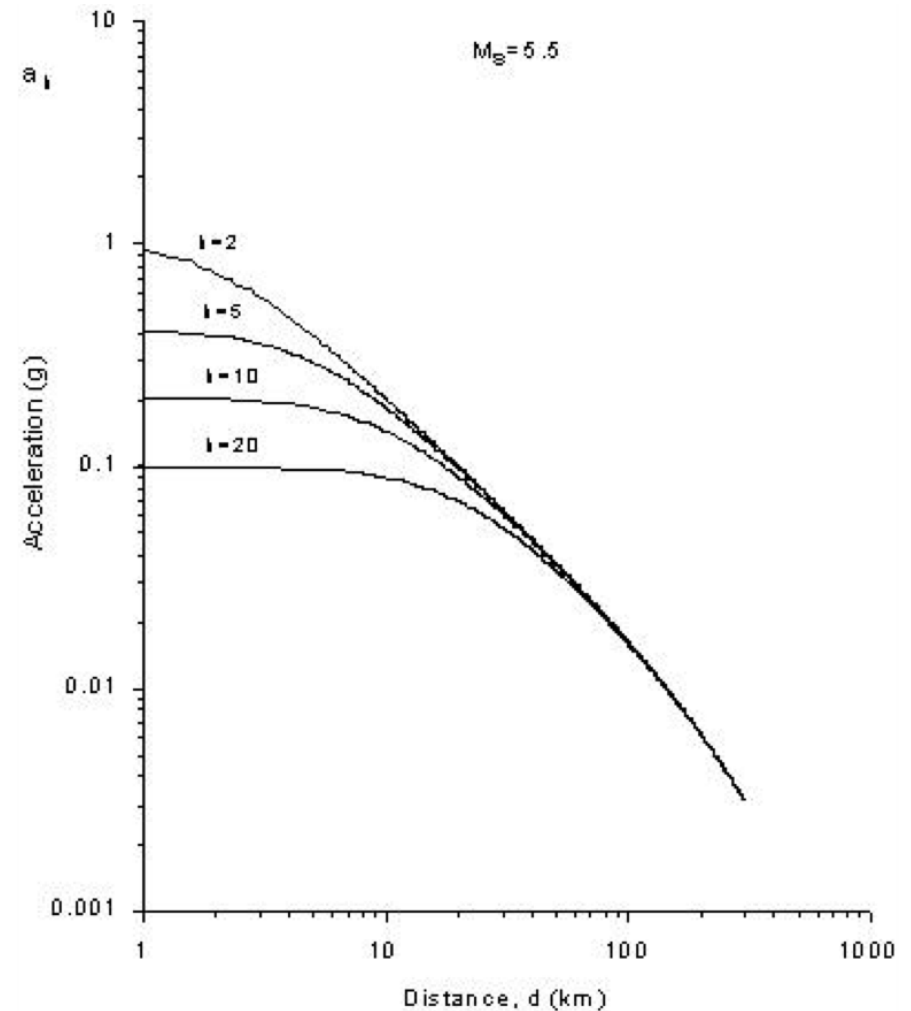
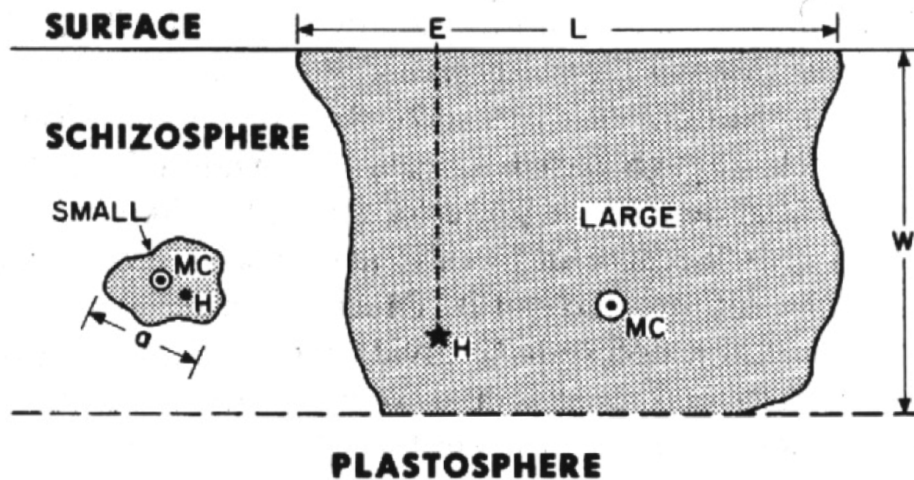


The selection of an appropriate distance matrix has a significant impact on the computed ground motion in the **near-field**

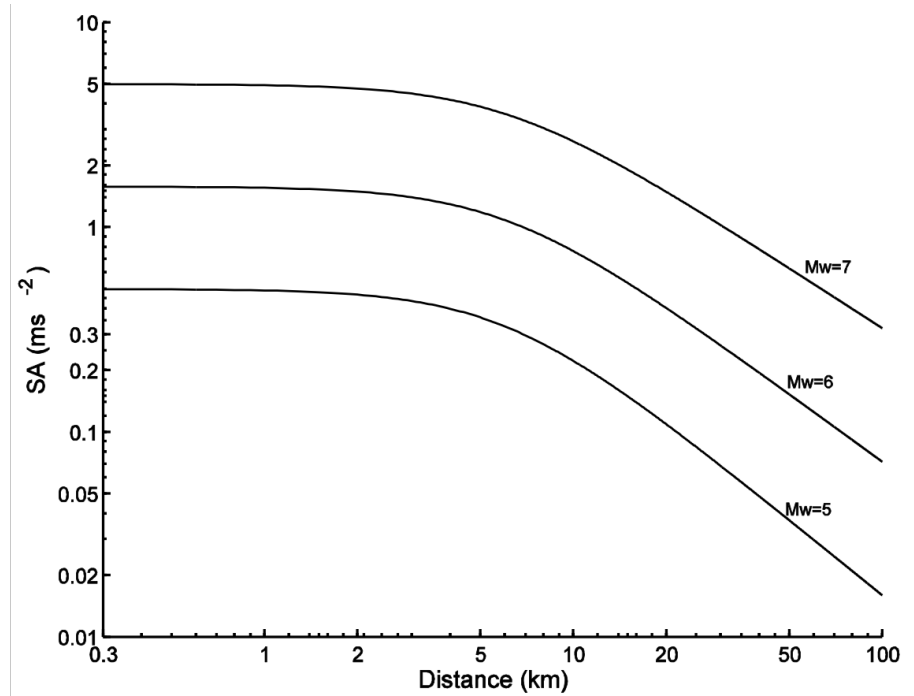
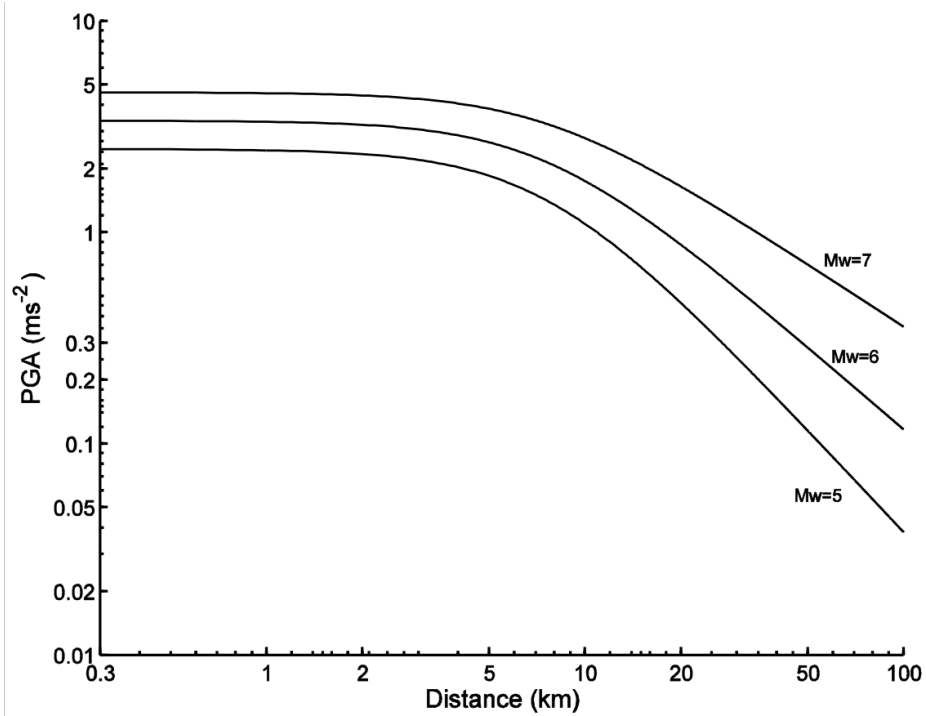
Focal Depth

Focal depth only has physical significance, for small crustal earthquakes

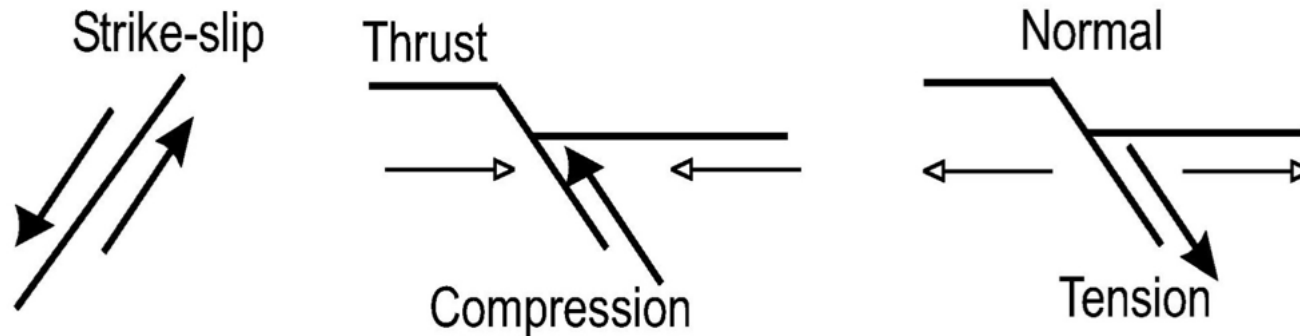
For small earthquakes can be dominant factor at short distances



Relation to Period



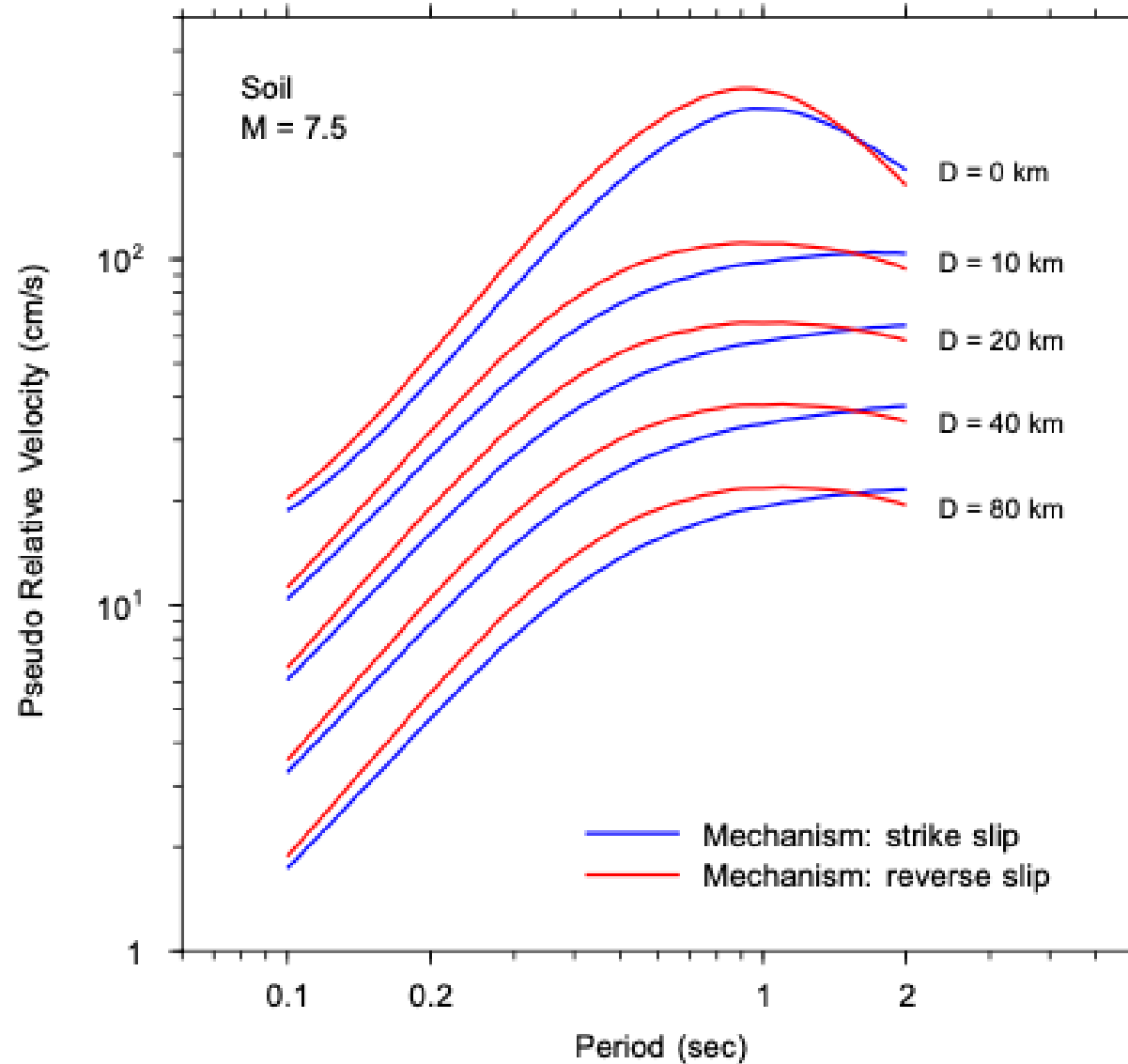
Effect of Faulting Style



Empirical observations show some differences in the levels of ground motion produced by reverse (R), normal (N) and strike-slip (SS) events.

- Most recent equations model difference between reverse and strike-slip
- Few equations model difference between normal and strike-slip
- Still uncertainty and no common agreement in size of such effect

Effect of Faulting Style

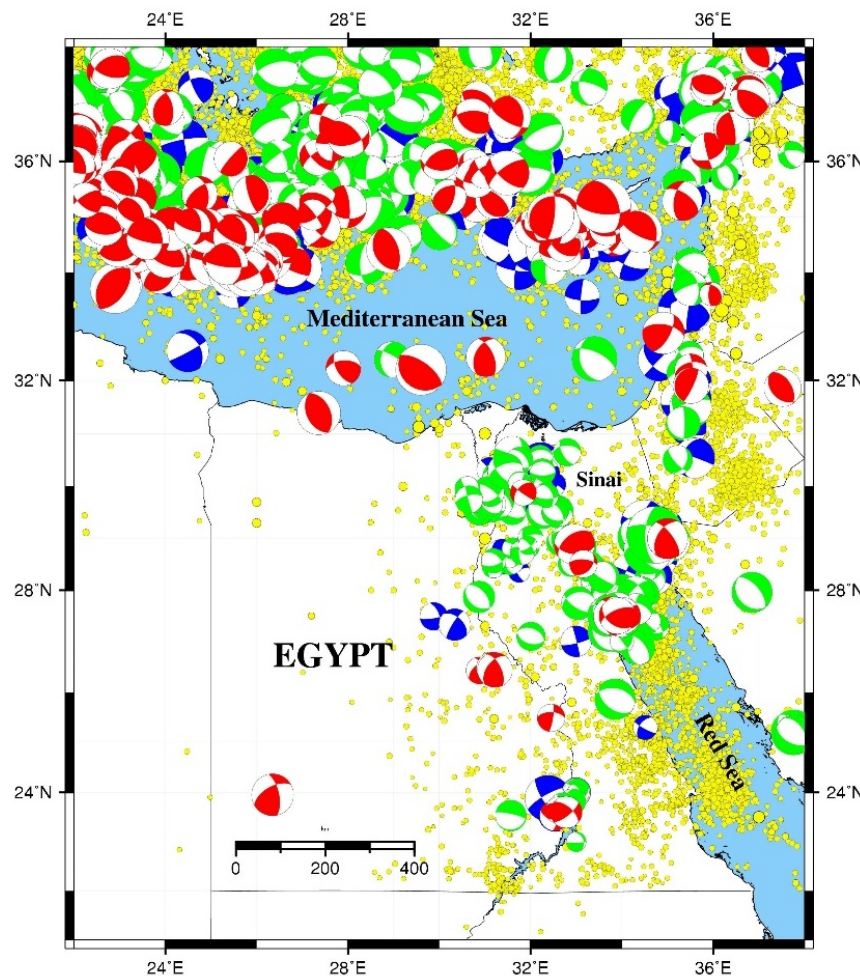


file:///C:/Users/poggi/Desktop/Engineering_Seismology_and_Seismic_Hazard/Chapter_10/10_10_08

Effect of Faulting Style

Faulting mechanism is related to the crustal stress, therefore major tectonic domains usually have a predominant mechanism.

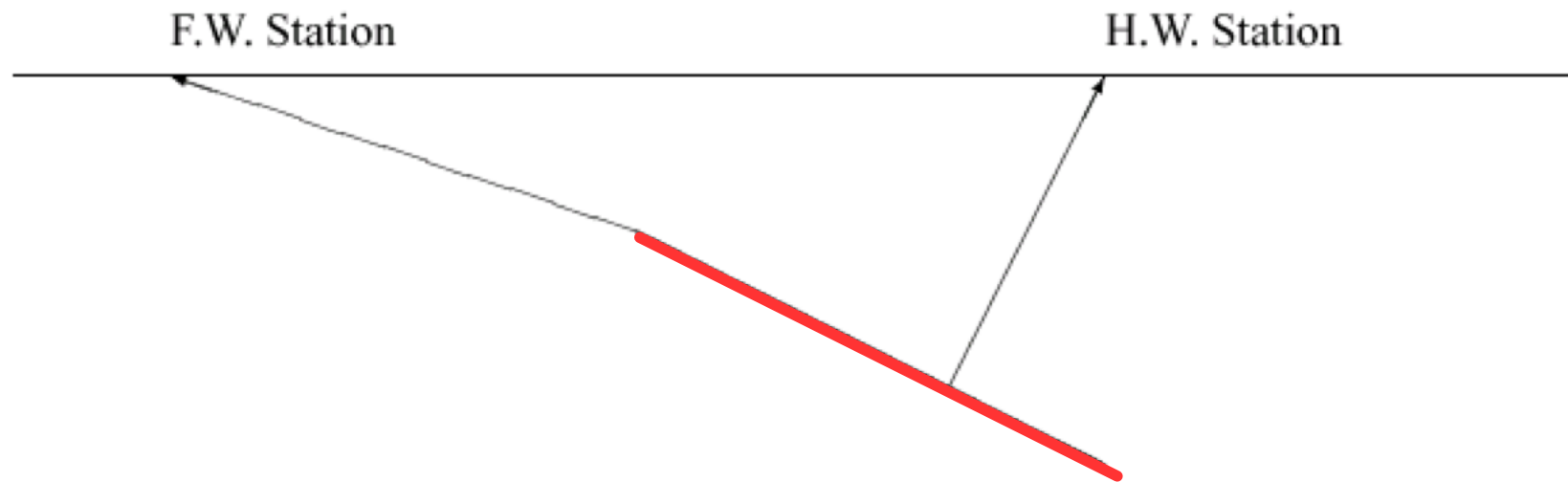
Regionalization is therefore important in GMPEs



Normal
Reverse
Strike-slip and oblique

Hanging Wall Effect

Sites located above the fault rupture on the hanging wall will have larger ground motions than sites at the same rupture distance located on the footwall because the hanging-wall sites are closer to a larger area of the source than the footwall sites.



Observations documented an increase of up to 50% in PGA on the hanging wall close to the fault.

Site Effects

Low-velocity layers strongly affect ground motion:

- Impedance contrast amplification between bedrock and softer layers
- Resonance of soft layers (amplification and deamplification)
- High frequency attenuation (deamplification)

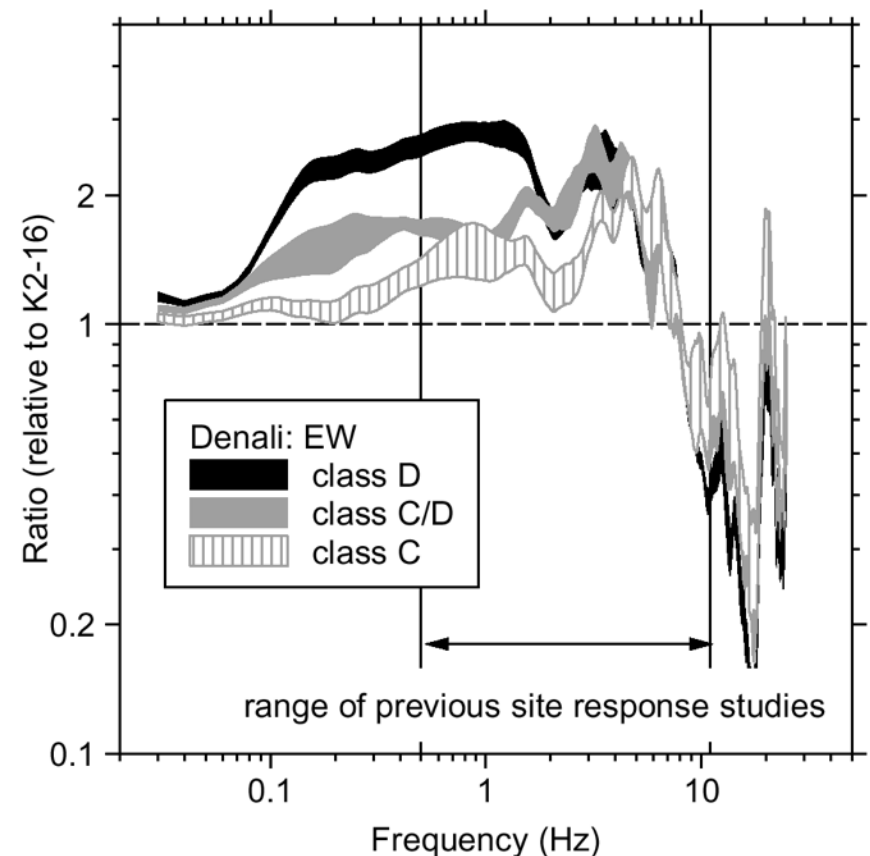
Different schemes as prediction variable:

- Soil classes (NEHRP, EC8, SIA)
- V_{s30} (continuous variable)
- Fundamental frequency of resonance (f_0)

TABLE 4.
Definition of NEHRP site classes (BSSC, 1994)

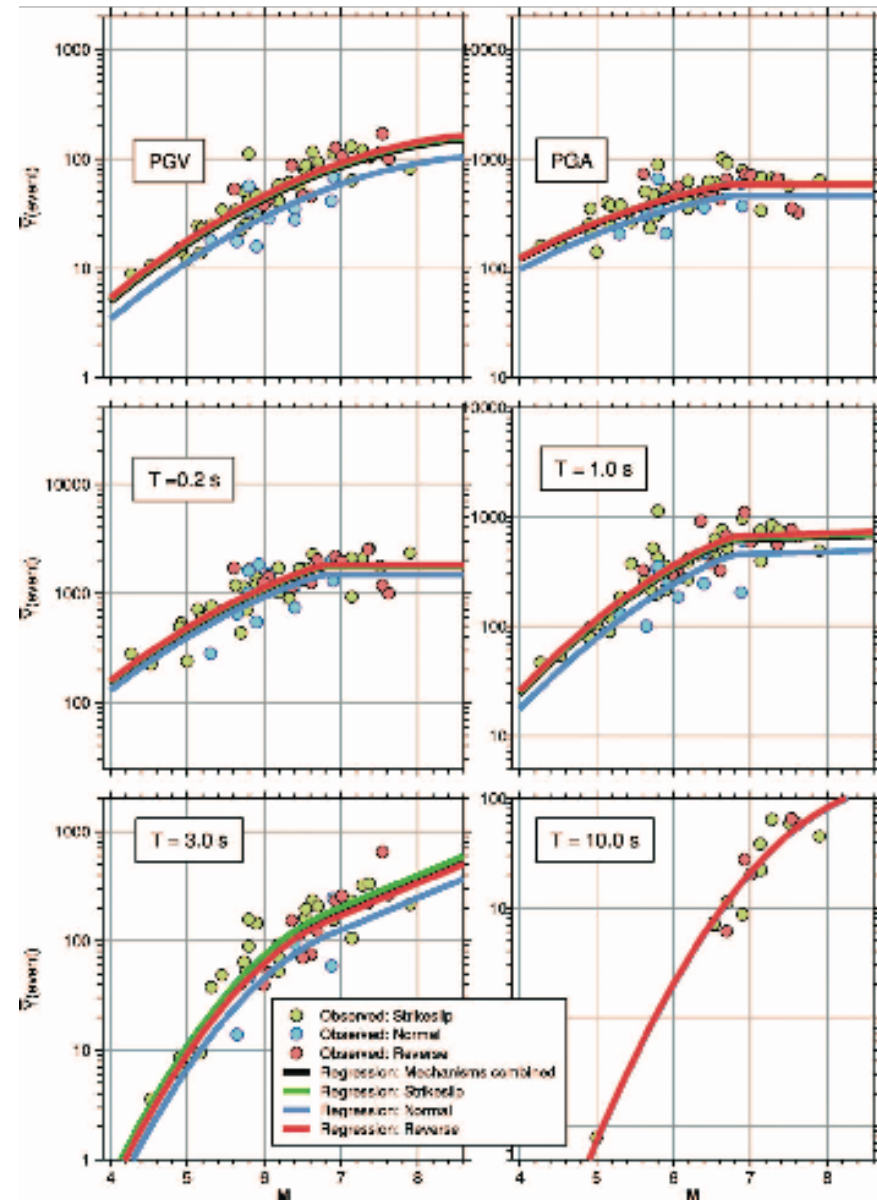
Site Class	Range of Shear Velocities*
A	greater than 1500 m/sec
B	760 m/sec to 1500 m/sec
C	360 m/sec to 760 m/sec
D	180 m/sec to 360 m/sec
E	less than 180 m/sec

* Shear velocity is averaged over the upper 30 m.



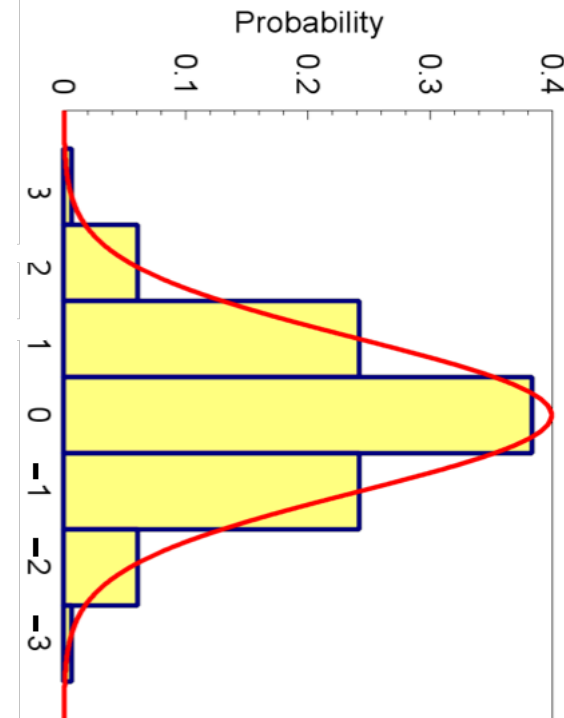
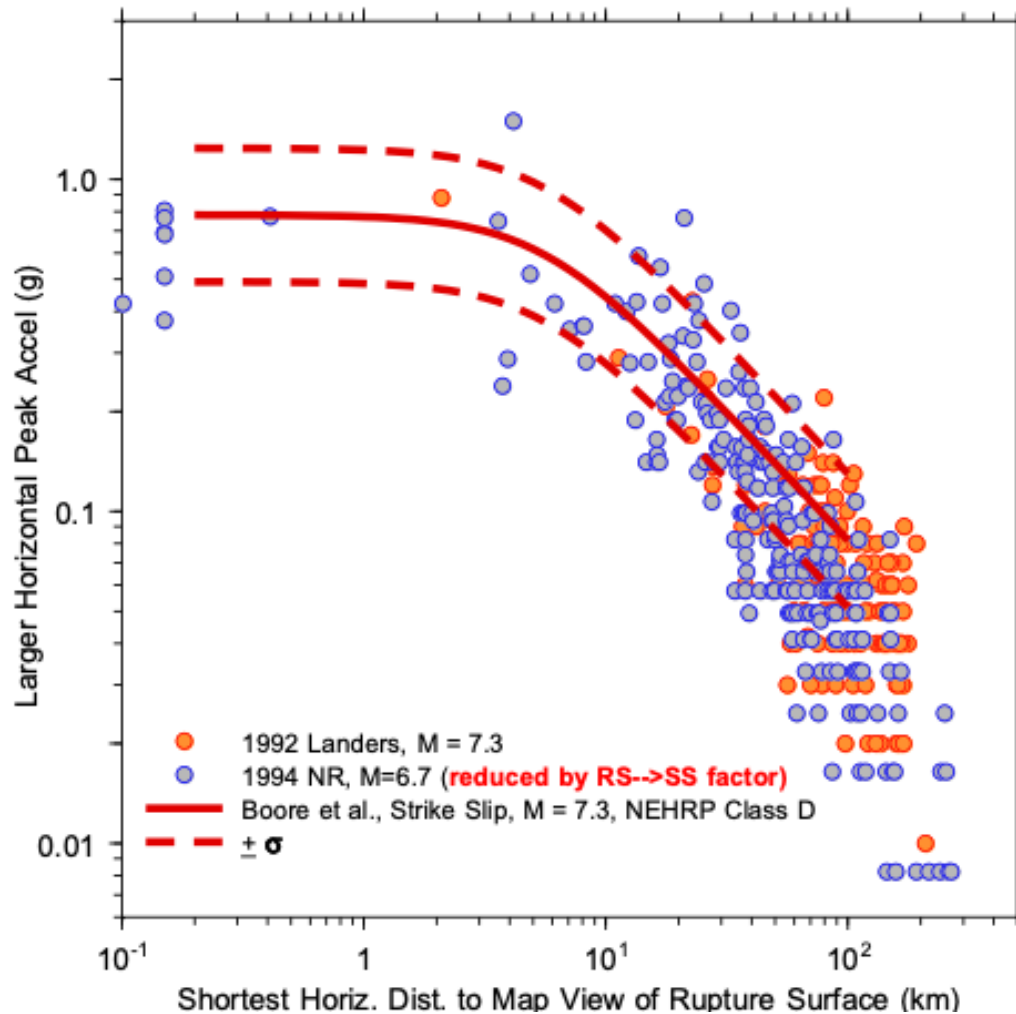
PGA Saturation

Recent GMPE functional forms incorporate the idea that high frequency ground motion saturates close to the fault (i.e. less dependent on magnitude than far from fault).



Aleatory Variability

Ground motion variability not captured by the relation is partially epistemic and partially aleatory.



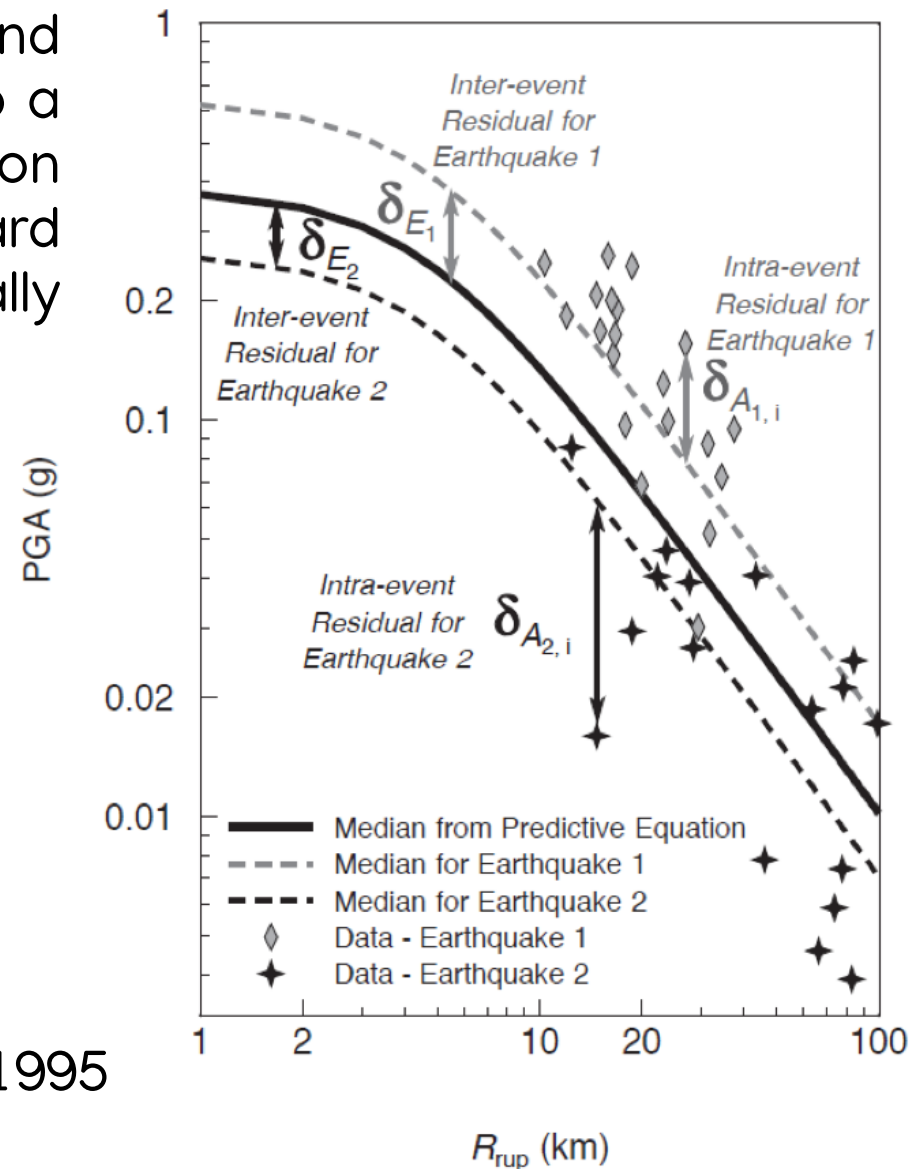
Uncertainty is assumed log-normally distributed

Aleatory Variability Components

The total variability of the ground motion σ is usually broken up into a between-events standard deviation (τ) and a within-event standard deviation (ϕ), assuming normally distributed.

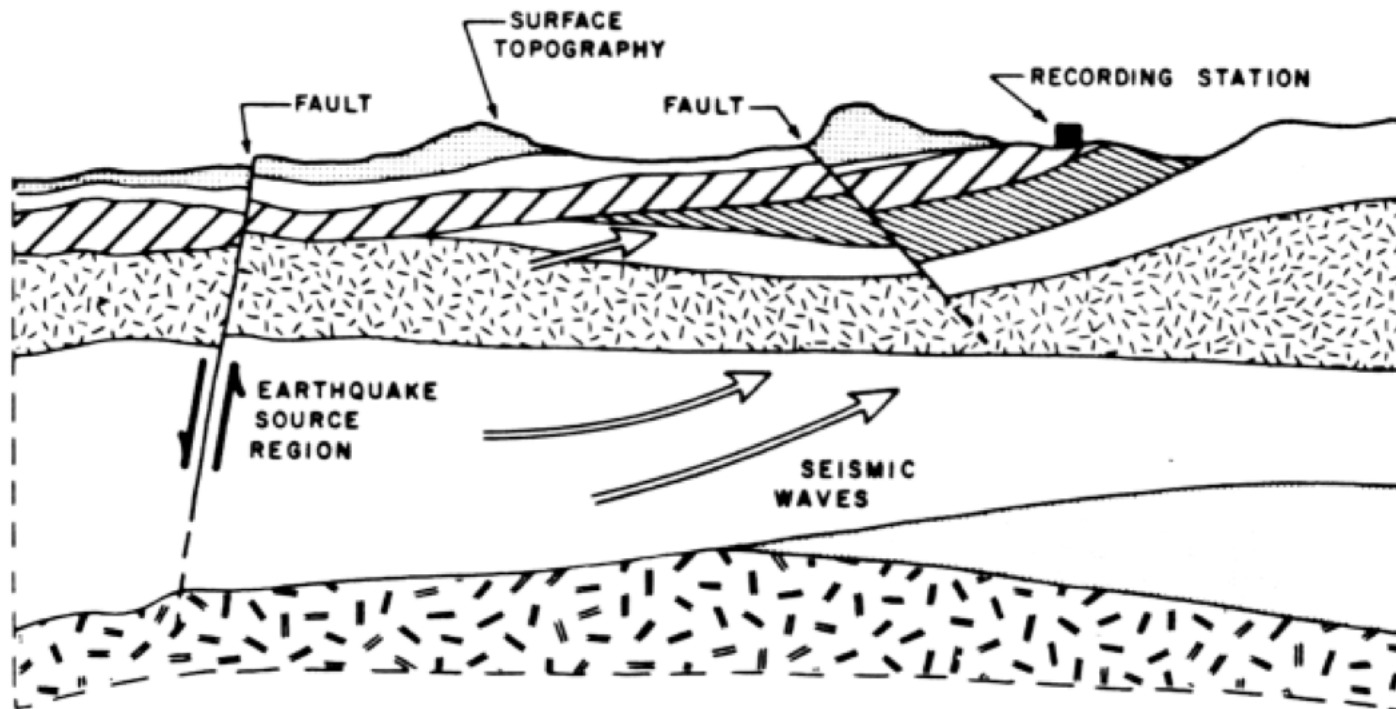
$$\sigma = \sqrt{\tau^2 + \phi^2}$$

Youngs et al., 1995



Cause of Uncertainty

- Observational not experimental
- Inappropriate independent variables
- Functional form too simple
- Unmodelled (or undocumented) source, path and site effects
- Poor or heterogenous datasets



Tectonic Regionalization

GMPEs are usually associated with a specific tectonic region; the use of a GMPE is generally recommended for a single TR.

First regionalisation of the world: Gutenberg and Richter (1954)

Major tectonic regions considered (Abrahamson and Shedlock, 1997):

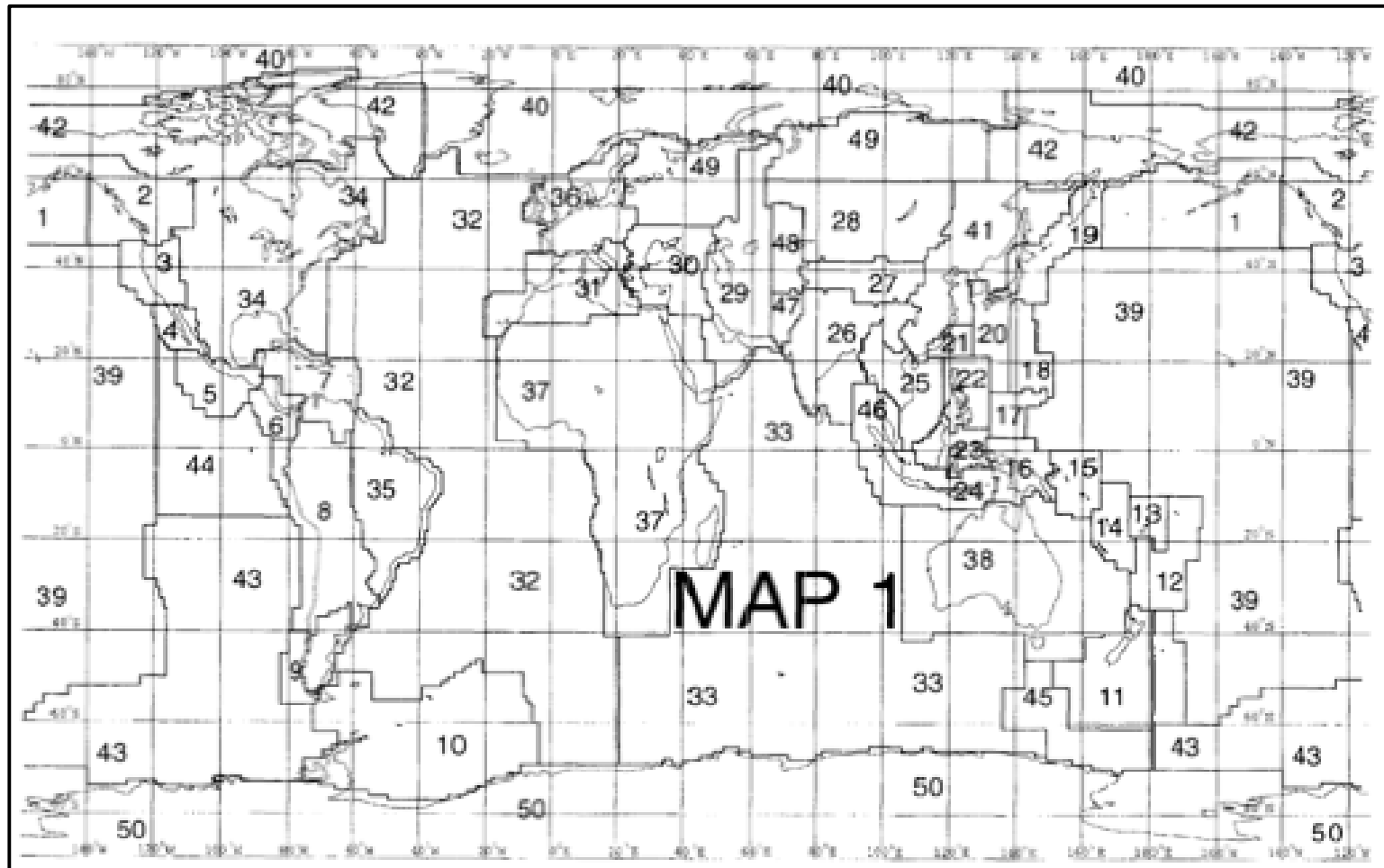
- Stable continental regions
- Subduction zones
- Shallow earthquakes in active tectonic regions

Regions lacking (or with a few) GMPEs due to the scarcity of recordings:

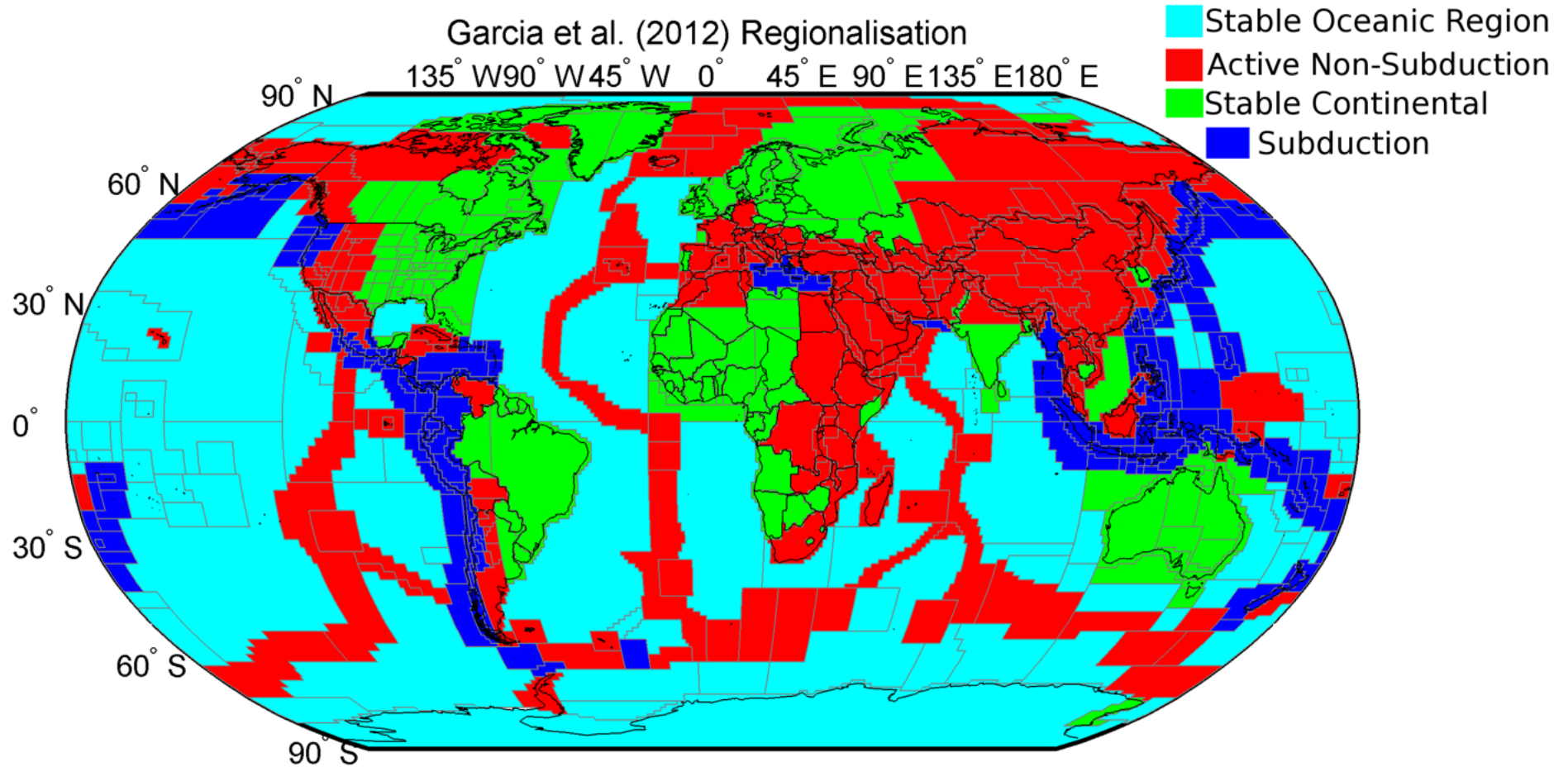
- Continental rifts
- Volcanic areas
- Deep events in active tectonic regions (e.g. Vrancea)

Tectonic Regionalization

Flinn-Engdahl regions proposed in 1965, mostly for earthquake localization. It follows political boundaries.



Tectonic Regionalization



Tectonic Regionalization

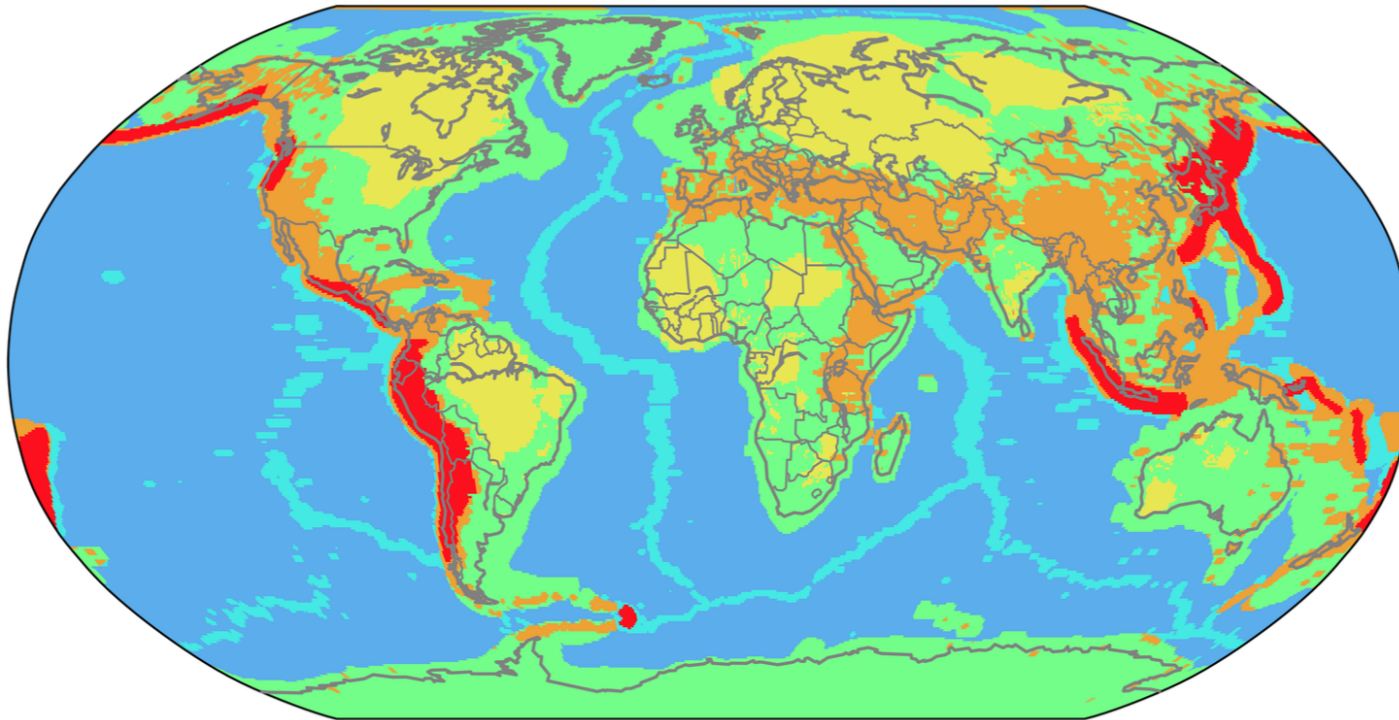
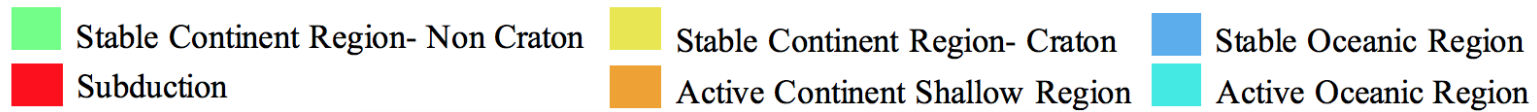


Figure 17. The maps shows the tectonic regionalisation model derived from our study for top 30 km.

Chen et al. 2017 – Merging information from:

- Seismicity (magnitude)
- Smoothed Moment rate
- S-wave velocity
- QLQ distribution

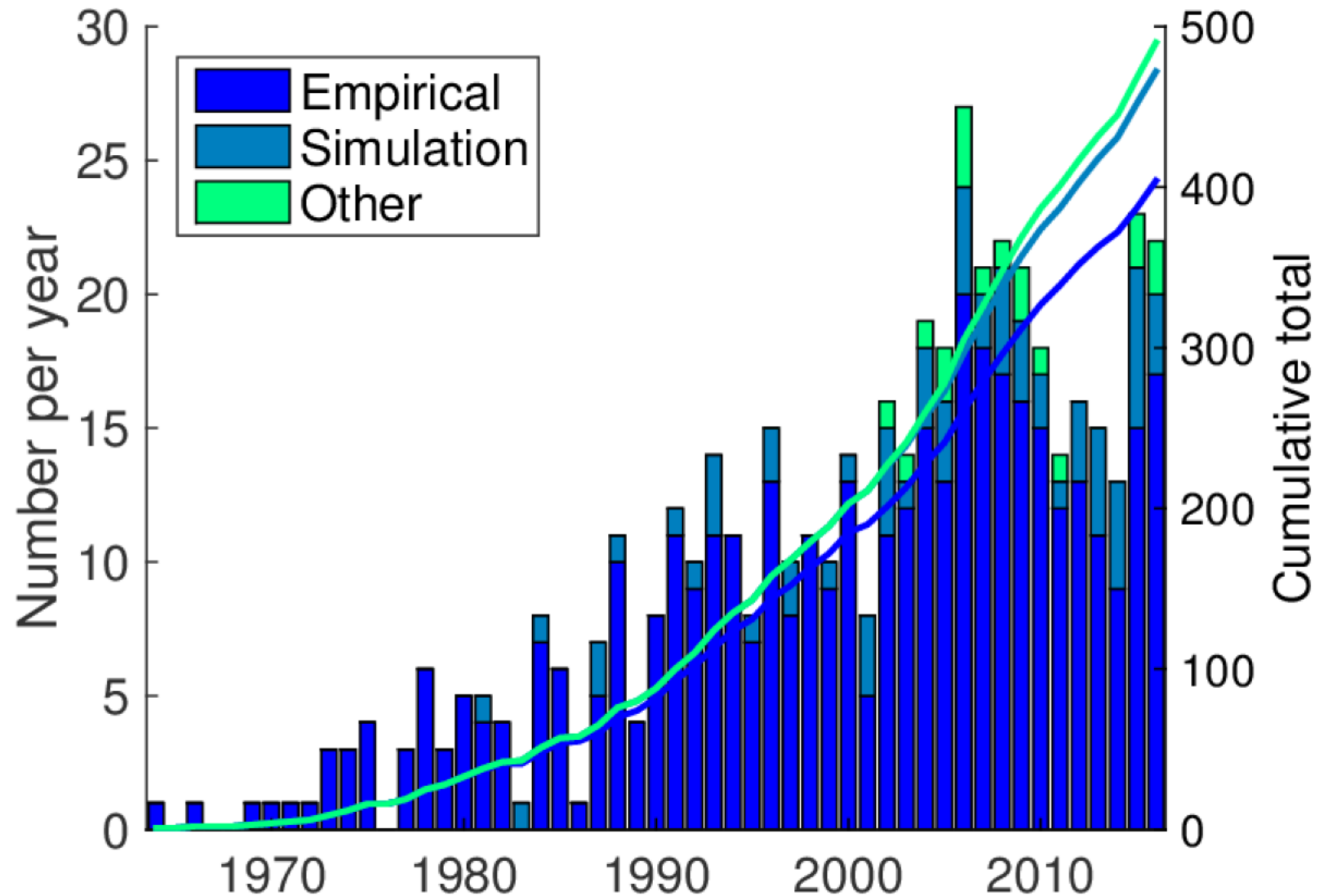
Current Standards

Summarizing, this is minimum requirement for a state-of-art ground motion prediction equation:

- Prediction variables: Geometric mean of PGA, PSA and PGV
- Processing: Low-cut filtering with record-specific cut-offs
- Source: M_w and normal/strike-slip/reverse categories, nonlinear M scaling
- Path: Joyner-Boore distance or rupture distance, M -dependent decay
- Site: $V_{s,30}$ or handful of $V_{s,30}$ -based site classes (e.g. EC8)
- Derivation: Random-effects/Maximum-likelihood regression
- Sigma: Between- and within-event sigmas

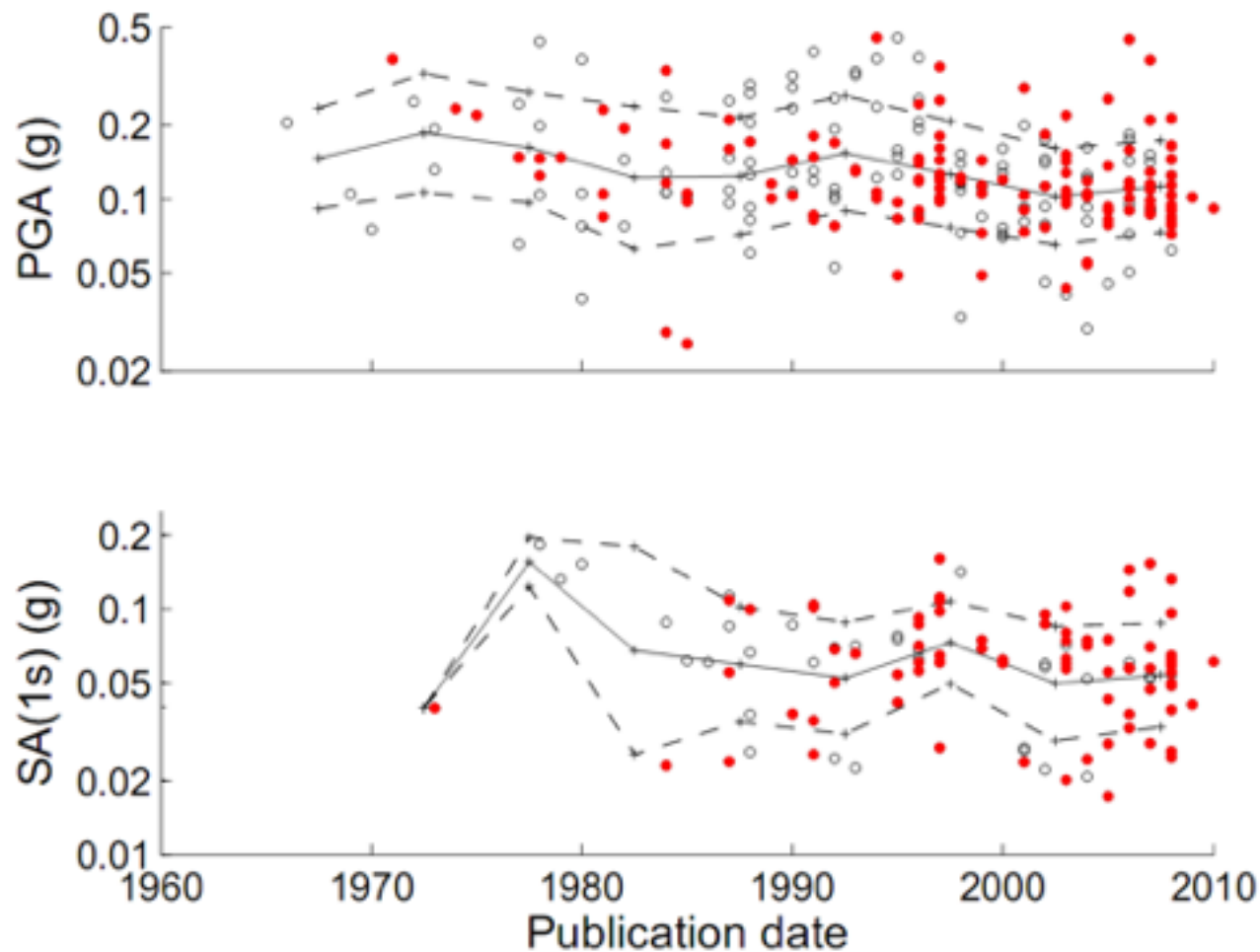
Would you like to make your own GMPE???

Number of Published GMPEs



Decreasing Uncertainty (?)

Although the many GMPE and recent developments, uncertainty did not significantly decreased over the years.



GMPE Selection Criteria

For regional hazard study it not practical to implement a new GMPE each time. Existing relations must be used.

But how to select the proper GMPE?

A) If local data available (not common):

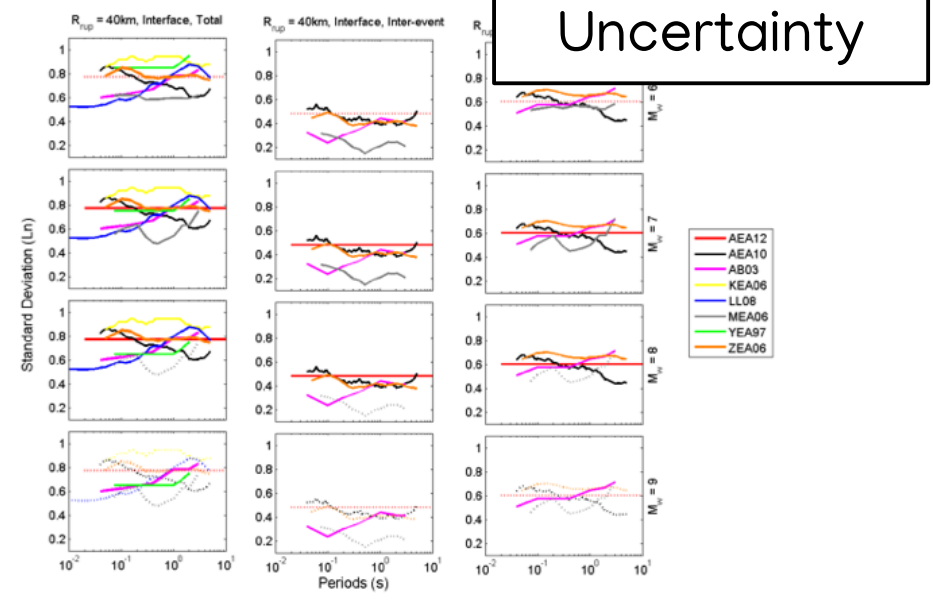
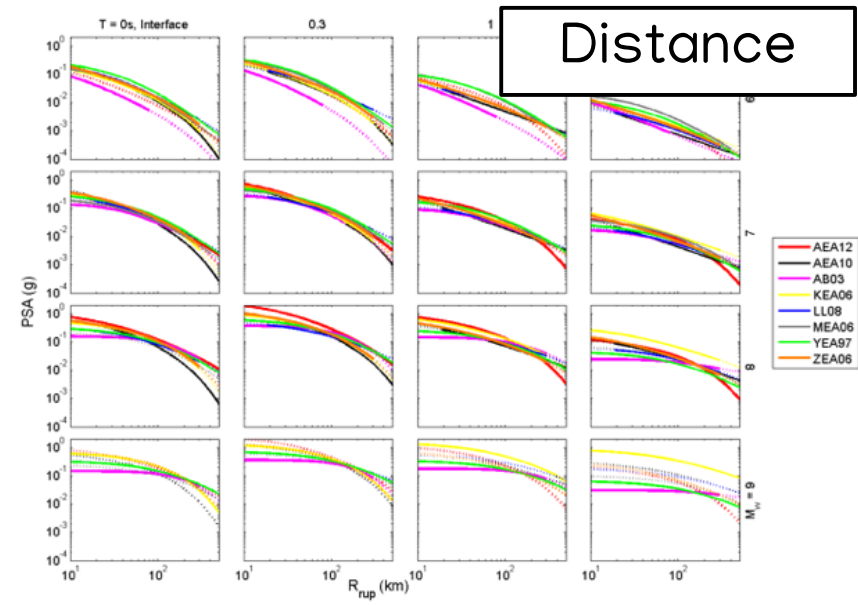
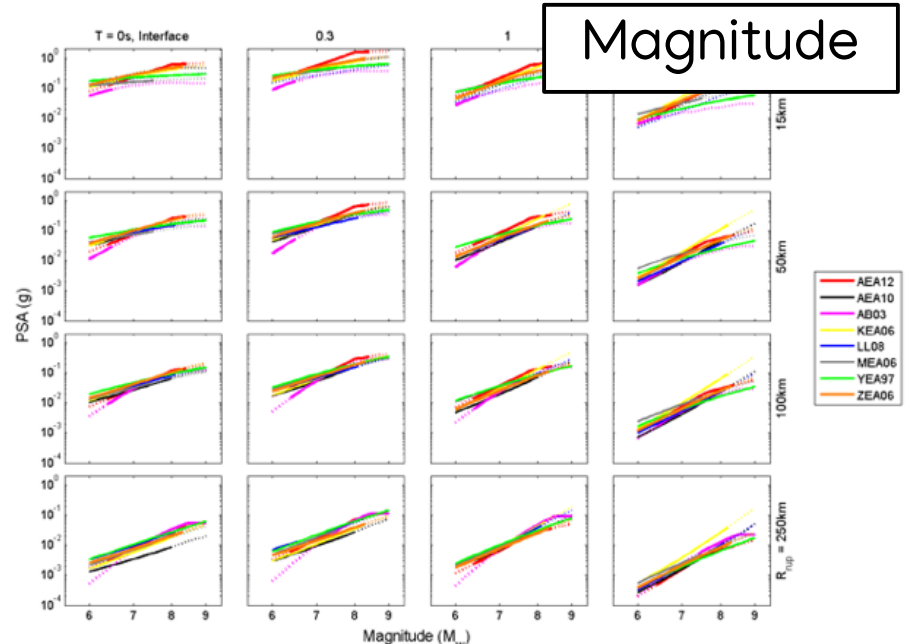
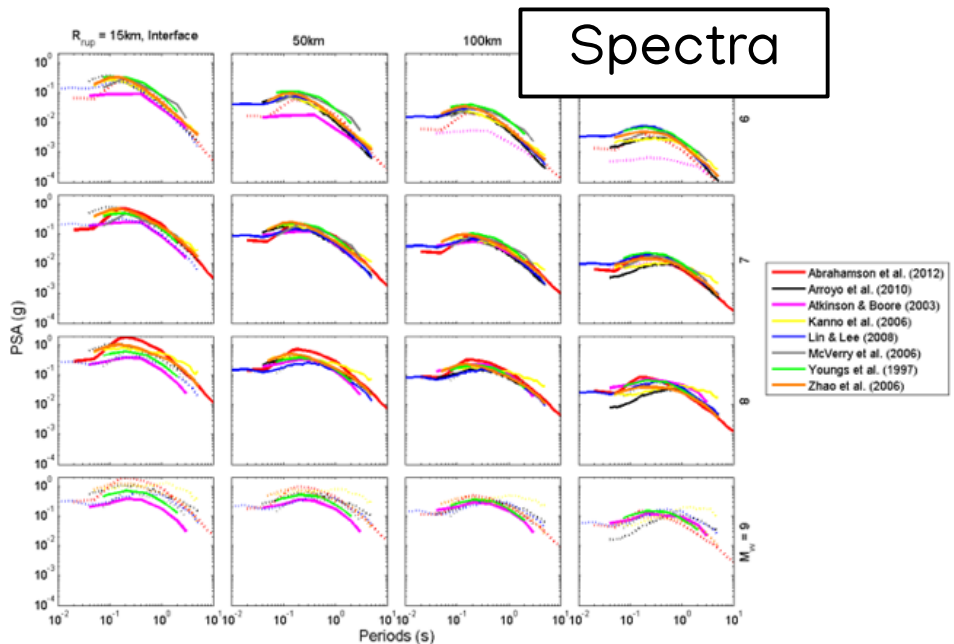
→ Compare and select the best matching GMPE

B) If data not available (most cases):

→ Select best GMPE based on indirect criteria
(e.g. Cotton et al 2006)

- Similarity of region type
- Robustness of calibration data
- Suitability of functional form
- Is state-of-art

Selection: Trellis Plots



Selection: Helpful Resources

Douglas 2019

Ground motion prediction equations 1964–2018

John Douglas
Department of Civil and Environmental Engineering
University of Strathclyde
James Weir Building
75 Montrose Street
Glasgow
G1 1XJ
United Kingdom
john.douglas@strath.ac.uk
<https://www.strath.ac.uk/staff/douglasjohndr/>

Wednesday 20th February, 2019

GEM's
HazardLib

openquake 3.4.0 documentation » openquake.hazardlib package » [previous](#) | [next](#) | [modules](#) | [index](#)

Table Of Contents

- openquake.hazardlib.gsim package
 - Ground-shaking intensity models
 - abrahamson_2014
 - abrahamson_2015
 - abrahamson_silva_1997
 - abrahamson_silva_2008
 - afshari_stewart_2016
 - akkar_2013
 - akkar_2014
 - akkar_bommer_2010
 - akkar_bommer_2010_swiss_coefs
 - akkar_cagnan_2010
 - allen_2012
 - allen_2012_lpe
 - armenia_2016
 - atkinson_2015
 - atkinson_boore_1995
 - atkinson_boore_2003
 - atkinson_boore_2006
 - atkinson_macias_2009
 - base
 - berge_thierry_2003
 - bindi_2011
 - bindi_2014
 - bindi_2017
 - bommer_2009
 - boore_1993
 - boore_1997
 - boore_2014
 - boore_atkinson_2008
 - boore_atkinson_2011
 - bradley_2013
 - bradley_2013b
 - campbell_1997
 - campbell_2003
 - campbell_bozorgnia_2003
 - campbell_bozorgnia_2008
 - campbell_bozorgnia_2014

Title

Text